AN ABSTRACT OF THE THESIS OF

Jesse A. Grimes for the degree of Master of Science in Mechanical Engineering presented on September 23, 2013.

Title:

ATRIAS 1.0 & 2.1: Enabling Agile Biped Locomotion with a Template-Driven Approach to Robot Design

Abstract approved: _____

Jonathan W. Hurst

Practical bipedal robots need to be simultaneously efficient, robust, and versatile machines, but designing robots dynamically capable of these demands has been a significant bottleneck. We designed ATRIAS to be a highly dynamic biped capable of both walking and running untethered in real environments. To meet these goals, ATRIAS is designed to approximate dynamically capable locomotion template, *i.e.* the *spring-mass model*. We enumerate the challenges of this template-driven design approach and our solutions to make ATRIAS a real-world-viable human-scale machine. We show that ATRIAS exhibits behaviors predicted by spring-mass models in fulfillment of our design approach. Particularly, ATRIAS reproduces the characteristic ground-reaction forces of human walking and running, a key dynamical feature of spring-mass locomotion.

We also demonstrate ATRIAS' capacity to walk, hop on one leg, bound like a spring-mass hopper, and recover from an unseen plunge into a 6.5-inch-deep gravel pit. Further, by building efficient spring-mass dynamics into the mechanical system, ATRIAS, when pushed, walks several steps without its actuators replenishing lost mechanical energy. These combined hardware experiments validate ATRIAS' capability as a platform for spring-mass robot controllers and for agile and economical locomotion in general.

This thesis is the combination of two journal papers that focus on the ATRIAS robot that focus on statements in the above paragraph. It also includes a summary of the objectives and considerations that went into the design, manufacture and testing phases of the robots. This includes the project deliverables and deadlines, methods for building these robots, control theory considerations for ATRIAS, engineering objectives and questions addressed by this work.

ATRIAS 1.0 & 2.1: Enabling Agile Biped Locomotion with a Template-Driven Approach to Robot Design

by

Jesse A. Grimes

A THESIS

submitted to

Oregon State University

in partial fulfillment of
the requirements for the
degree of

Master of Science

Presented September 23, 2013
Commencement June 2014

Master of Science thesis of Jesse A. Grimes presented on September 23, 2013.

APPROVED:

Co-Major Professor, representing Mechanical Engineering

Co-Major Professor, representing Mechanical Engineering

Head of the School of Mechanical Industrial and Manufacturing Engineering

---

Dean of the Graduate School

I understand that my thesis will become part of the permanent collection of Oregon State University libraries. My signature below authorizes release of my thesis to any reader upon request.

Jesse A. Grimes, Author

ACKNOWLEDGMENTS

I would like to thank my major adviser, Jonathan W. Hurst, for all of his guidance and support, my co-advisor, Irem Y. Tumer, for her support, my thesis committee, and my colleagues in the Dynamic Robotics Laboratory for their hard work, friendship and the willingness to listen to Metallica once and awhile. Thanks to the OSU Robotics Club and specifically the Mars Rover 2010 & 2011 teams for prepping me for real world robotics projects. In addition, I would like to thank my family for all their love and support, without whom this thesis would not exist.

Funding for this work was provided by the Defense Advanced Research Projects Agency (DARPA) and the Human Frontiers Science Program (HFSP).

CONTRIBUTION OF AUTHORS

Chapter 2 is a journal paper of which I wrote with one co-author, Hamid Reza Vejdani. Hamid's contribution to this work is the mathematical proof found in Appendix A

Chapter 3 is a journal paper of which I wrote with several co-authors, named here in alphabetical order by last name: Andy Abate, Christian Hubicki, Mikhail Jones, Daniel Renjewski, and Alexander Sprö witz. My contribution to this work is contained in Section 3.3.

TABLE OF CONTENTS

TABLE OF CONTENTS (Continued)

LIST OF FIGURES

LIST OF FIGURES (Continued)

LIST OF FIGURES (Continued)

LIST OF FIGURES (Continued)

LIST OF FIGURES (Continued)

LIST OF TABLES

LIST OF APPENDIX FIGURES

LIST OF APPENDIX TABLES

DEDICATION

Space, The final frontier. These are the voyages of the starship: *Enterprise*. Its continuing mission: to explore strange new worlds, to seek out new life and new civilizations, to boldly go where no one has gone before.

Chapter 1 – Introduction

1.1 The Purpose of ATRIAS

ATRIAS is a research platform developed for the implementation and testing of controller ideas and methodology for bipedal walking and running based around the spring-mass model framework. The goal of the platform is to achieve robust and energetic walking and running in full 3D with no added support or tether. The robotic platform is developed to match the spring mass model's *passive dynamics*, the dynamics of the system with no contributions from motors or other actuators, with the goal of testing ideas that were developed in simulation for the spring-mass model. This idea of having a legged robot that acts like a simple pre-defined model is novel in the robotic legged locomotion community and is the basis for the name of the robot: ATRIAS **A**ssume **T**he **R**obot **I**s **A** **S**phere.

The passive dynamics of the spring-mass model are inherently energy conservative. The inclusion of a series spring in the leg allows for a reduction in energy losing shockloads, furthermore all kinetic energy from the gait is stored during stance phase and returned while returning to flight phase. That is, the model includes no sources of loss for legged locomotion: friction, damping, etc.. Powerful actuators are included in the design of the robot for the purpose of having control authority to achieve a *robust* gait, one that overcomes significant disturbances.

1.2 Control Theory Considerations for ATRIAS

During the design of ATRIAS a specific set of control ideas were considered for use on ATRIAS, a method that can be summarized as: force control. The fundamentals of force control are that the forces interacting between the robot and the ground/environment can be controlled by the robot to achieve a desired task. In this case walking or running. In simulation it has been shown in literature that the spring-mass model can replicate these ground reaction forces as observed in legged biological systems [1–4]. To this end, ATRIAS is developed to be a high bandwidth force controlled actuator. Large plate springs are placed in series with the motors and the deflection of both are measured with very high resolution. Additionally the motors position is sensed with very high resolution so that the controller will have very good position and velocity measurements on which to make decisions and control the system. Thus, ATRIAS has the passive dynamics that exhibit the same ground reaction forces as observed in nature, and can control these forces for added gait stability and robustness.

1.3 Background for this Thesis

Of course other legged robots have been built to date, and even several have spring-mass characteristics similar to ATRIAS. But ATRIAS stands alone as a human scale spring-mass biped robot. Other spring mass robots to date include the ARL Monopod II [5], Bow Leg Hopper [6], and of course the Raibert hoppers [7]. These robots featured series compliance within their legs allowing for very dynamic

locomotion, yet these machines were all short compared to ATRIAS.

Other biped robots follow a very different philosophy from ATRIAS. Robots like ASIMO employ a walking strategy called Zero Moment Point (ZMP) where the robot's center of mass is always held above the foot in contact with the ground [8]. While this method of legged locomotion is successful, and results in a legitimate walking gait, the gait is not an order of magnitude greater in energy consumption compared to a human.

The state of the art in legged locomotion is the Boston Dynamics Big Dog and LS3. Both are quadruped robots capable of walking and running outside through brush, mud, ice, rocky areas, just about all you could hope for in a legged robot. The problem with these amazing machines is that they consume very high amounts of energy, more than ASIMO. Exact number can't be cited because Boston Dynamics doesn't publish enough information concerning the energetics of these robots. Our estimate here is based on the fact that they employ a gasoline motor to power a hydraulic system (15Hp for Bigdog and 75Hp for LS3). More recently, they have developed the Atlas robot, a humanoid, for the DARPA Robotics Challenge with the same design philosophy of its quadruped siblings.

1.4 Engineering Objectives and Questions

The engineering objectives and questions explored in this thesis is "given a spring-mass, template designed robotic leg, how does one configure two of these legs, add actuation to this new degree of actuation and pack on all the electronics

and components necessary for unsupported, tether-free locomotion?" From this we have two objectives: 1) hip adduction/abdcution actuator, 2) body for housing and protecting all components necessary for the robot to operate. The method for developing the hardware implemented on ATRIAS 2.1 is described in the following subsection.

With the above goals for the robot, the time line for delivering two of the three robots was set for one year from the decision to build the three bipeds. This set of deadlines was ambitious and required a great deal of work to make a reality.

1.5 Methods

The method employed in the work of this thesis is a combination of analysis, design and prototyping prior to the final construction of the ATRIAS robot. The key design aspects of ATRIAS were developed by Dr. Jonathan Hurst prior to my arrival in his research lab (the Dynamic Robotics Lab) and my place was to finish design details of the ATRIAS leg, and develop the lateral actuator and body for the biped configuration of ATRIAS. To this end, the concept of these aspects of the robot were developed and many design iterations were evaluated prior to the construction of the prototype that is named ATRIAS version 1.0. The lateral actuator and body designs were not complete at this point and required a great deal of analysis and further designing, however, the decision was made to build the best design on hand due to the impending construction of the prototype leg (version 1.0) which was ready for prototyping. For the leg to interface with the

support boom there was need for a lateral actuator. The decision was based on the fact that as much or more could be learned from prototyping the lateral actuator than could be learned from further analysis without the prototyping in the same amount of time. Thus the creation of the first version of the lateral actuator and body.

The major revision stemming from what was learned with the prototype lateral actuator was that the location of series compliance was erroneous. As discussed in Chapter 3, the series compliance was located between the mass of the leg motors and the body. This resulted in large, difficult to control oscillations; undesired behaviour. The correction implemented in the later prototype and final version of ATRIAS was relocating the series compliance within the leg (below the mass of the leg motors). Sensors were included to measure this compliance to the effort of controlling the deflection to a desirable amount (force control). To this date, however, engineering testing has not been completed to find out how well suited this idea is for the lateral actuator (hip adduction and abduction) for a biped robot.

The body design of ATRIAS was developed through two prototyping iterations before the final design. The goal of the body is to house and protect all of the components necessary for the robot to operate. This includes: batteries, computer, distributed microcontrollers, motor amplifiers, inertial measurement units. The first prototype was lacking in completion and protection for internal components due to reasons stated above. The second prototype was a completed design with all components enclosed and accounted for. The final design improved the protection

of these components

1.6 Introduction to Chapter 2

The first journal paper included in this thesis work is presented in Chapter 2. This paper introduces the mechanical design concept of ATRIAS to the scientific community. It details in depth the mechanical design and how all major features work to achieve a robot capable of hopping. The appendix of this paper features a mathematical proof of the dynamical match between the ATRIAS model and the spring-mass model which was written by co-author: Hamid Reza Vejdani. As of the completion of this thesis the paper is submitted to the journal: Elsevier, Mechanisms and Machine Theory.

1.7 Introduction to Chapter 3

The second journal paper included in this thesis work is presented in Chapter 3. This paper continues from the previous paper and details results from the completed biped configuration of ATRIAS. New and completed aspects of the design such as the body and lateral actuator are introduced. My contributions to this paper lie in Chapter 3, Section 3.3. The remaining contributions are from my co-authors whose primary purpose was to validate the design criteria of the robot and prove that it does indeed match the intended dynamics of the spring-mass model. Further, demonstrations are included showing that the robot has the

capability to walk and run dynamically. Future work will build on this work taking the walking and running to new heights of robustness and energetics. This paper is not submitted as of the completion of this thesis, but is intended to be submitted to the International Journal of Robotics Research (IJRR).

Chapter 2 – ATRIAS 1.0: Design and Demonstration of a Spring-Mass Hopping Robot in Human Scale

In this paper we describe ATRIAS, a monopod robot designed specifically to match the key dynamic features of the spring-mass model while also providing ample actuation authority. The goal of building this robot is to enable the investigation and application of control methods that utilize the spring-mass framework to approach the robust and energy economical performance seen in animals. We describe the hardware design as it relates to matching a desired *dynamic* model rather than achieving a desired *kinematic* model, including a four-bar linkage leg, a novel cable drive transmission, the implementation of springs in series with electric actuators, and other defining features of the machine. The paper concludes with a discussion of concepts and design elements that worked well, and ideas that required revision.

2.1 Introduction

We present the design of ATRIAS 1.0, a spring-mass monopod robot that is a prototype for eventual 3D, outdoor locomotion (Figures 2.1 and 2.2). ATRIAS is a model-based robot, meaning that the passive dynamics (the behavior of the un-

actuated system) are designed to behave like an easily understood dynamic model. This philosophy is the basis for the acronym ATRIAS: Assume The Robot Is A Sphere. The model is defined before the first design sketches are drawn: a spring-mass system, as shown in Figure 2.3(a). A spring-mass model is appropriate for several reasons: First, it describes observed features of animal walking and running, which remain our best example [9]; second, there is extensive theoretical background work on controls for mass-spring systems, which shows very efficient, robust gaits and self stability [10–18]; third, it is possible to build a robot to match this system closely, with few compromises. This approach enables controllers that ignore mechanical complexities, and rely on the passive dynamics of the simple model as an integrated part of the combined mechanical-electrical-software dynamical system. ATRIAS 1.0 successfully demonstrated the spring-mass hopping behavior, shown in Figure 2.2.

Walking and running gaits are dynamic behaviors resulting from complex interactions between passive dynamics of a mechanism and active control. In traditional control methods, the system dynamics are referred to as the "plant", and a simple first step in writing control software is to invert the plant dynamics and attempt to cancel all of the passive behaviors, so the desired behavior can be implemented entirely via software control. However, this approach is ill-advised for legged locomotion, due to inherent physical constraints such as actuator torque limits and inertia. Furthermore, legged locomotion involves regular impacts, significant amounts of energy transfer in a cyclic manner, and very high momentary power requirements. For realistic systems it is extremely challenging, if not im-

(a) (b)

Figure 2.1: (a) ATRIAS 1.0 completed prototype robot. (b) ATRIAS 1.0 Solidworks model.

Figure 2.2: Stroboscopic image created from video of ATRIAS 1.0 maintaining a hopping gait. Center of mass path is traced for example only and is only qualitatively representative of the actual gait.

possible, to create actuators that can adequately deal with all of these factors. Instead, our approach to legged locomotion is to co-design the mechanism and the software control such that they cooperate to achieve the desired behavior. This approach mirrors animal neuro-mechanical systems in creating the best examples to date of efficient, robust legged locomotion.

While a machine cannot perfectly match a spring-mass model because of unrealistic requirements such as a massless leg, it can come sufficiently close that spring-mass control methods can be applied. ATRIAS 1.0 has a center of mass near the hip, like the spring-mass model; legs that comprise less than 5% of the robot mass; physical springs in the leg length direction; and accurate sensing and

a backlash-free transmission for near-ideal actuation and control.

This paper focuses on the design details and justification for how this implementation of the ATRIAS leg configuration relates to the spring-mass model, and what lessons we learned. Discussion will include: how ATRIAS approximates the spring mass model; important and noteworthy details of the ATRIAS leg configuration; the extension of the planar spring-mass model into 3D with the inclusion of lateral actuation; the planarizing robot support boom; and mechanical design details of the compound epicyclic cable drive transmission. We also discuss recommendations based upon these lessons learned that will be applied towards tether-free, 3D, efficient, robust bipedal walking and running robots.

2.2 Background

To fully understand the reasoning for choosing the spring-mass model as the basis of ATRIAS one must understand the significance of this model to legged locomotion. Here we present these key ideas about the spring mass model as well as past robots that capture some of these ideas.

2.2.1 Why the Spring-Mass Model?

A simple spring-mass model, such as that shown in Figure 2.3 (a), has been shown to approximate the center of mass motion during *steady running gaits* of a wide diversity of terrestrial animals, regardless of the number of legs, body size, or anatom-

ical detail [10, 19–24] better than competing models, such as the the compass gait [25–28], the "simplest possible" model [29,30], or the seven-link biped [31–33]. As a result, spring-mass models have become the foundation for much of the research on running, implicitly or explicitly. Significant theoretical work has been done analyzing the dynamics and stability of the model [34–39]. Successful running robots such as the Planar Hopper [7], ARL Monopod II [5] and CMU Bowleg Hopper [40] exhibit spring-mass behavior, and most likely were designed specifically to do so. In addition to running gaits, the same spring-mass model arranged in a bipedal pair has also been shown to reproduce steady-state dynamics of human walking [41]. This finding implies that walking and running are basically two different harmonics of the same spring-mass system.

2.2.2 Integration of Passive Dynamics and Active Control

Although running animals use a 'bouncing' gait pattern that is consistent with a completely passive spring-mass model, it is actually achieved through an as-yet unclear combination of passive compliance and active control by muscles [42–45]. There have been many techniques for controlling or stabilizing under-actuated systems [46–50], and some have specifically embraced the passive dynamics [51,52]. However, actuation is a requirement, as internal friction and collision losses in physical systems require energy input to maintain a consistent gait.

Actuating a spring mass robot by placing motors in series with the spring enables good force control [53]. Force control during stance is potentially use-

ful for controlling gaits in uncertain environments, and has been demonstrated in walking over unexpected ramps [54] and running [55]. Force control methods for spring-mass walking and running have been shown to reproduce observed animal behaviors previously interpreted as stiffness adjustment, suggesting that animals may control ground reaction forces actively to maintain a passive-like stance behavior even over terrain that changes impedance and height unpredictably [56–60]. The configuration of a spring in series with an actuator mirrors the muscle-tendon unit in animals, lending credibility to the hypothesis. ATRIAS will be capable of replicating this force control behavior to stabilize gaits.

Placement of springs in series with the motors is not only good for implementing force control, but also allows for impact tolerance and reduces motor work compared to both parallel spring and direct-actuation configurations. At each footfall during any gait there is an inelastic collision with the ground; inertias associated with leg mass lead to significant energy losses and impact forces. If an actuator is rigidly connected to the leg, as in most humanoid robots, the reflected inertia associated with the actuator is often on the scale of the robot mass, and thus ground impacts become a major problem. Such robots tend to handle ground impacts poorly, and often carefully approach the ground to minimize impact forces. This caution is one reason such robots cannot handle unpredictable, outdoor environments. The addition of a series spring addresses the fundamental problem - a parallel spring, however, does not, because the actuator must track the output of the leg and spring, and is still subject to impact forces, both costing energy. Further, a motor in parallel with a spring must work against the spring to move

the leg, a source of energy loss for every step during a gait.

2.2.3 Robots

The balance of passive dynamics and active control that animals and robots use in their motions has significant consequences for economy, agility, and disturbance rejection performance. Most robots use control that attempts to overcome passive dynamics to achieve desired endpoint trajectories, resulting in poor handling of impacts and low energy economy. Examples include current humanoid robots, such as Honda's Asimo and Toyota's Humanoid robot. These machines can walk and run according to the dictionary definitions of "walk[1]" and "run[2]," but the gaits are significantly different from animal gaits and significantly less efficient.

At the other end of the spectrum, some walking machines are entirely passive, and include no electronics or actuation whatosever [61]. The Cornell Walker uses an absolute minimum of active control to maintain a rigid-leg walking gait, relying almost entirely on passive dynamic behaviors [62, 63]. This approach leads to great efficiency, as demonstrated by the robot's 40-mile walk on a single battery pack. However, it is very sensitive to disturbances, and walked in a gymnasium to avoid rough terrain. While the active machines use methods like Zero-Moment Point (ZMP) control to move their center of mass forward [8,32,64,65], the passive machines are explicitly based on the inverted pendulum model and its passive

[1] An incomplete yet common definition for *walking* is an "alternating series of single support and double support phases"

[2] An incomplete yet common definition for *running* is "an alternating series of stance and flight phases"

dynamics [66, 67]. For most machines, the passive dynamics are not quite ideal, and virtual constraints can be used to reduce the order of the robot model, or to match an idealized model for control purposes [68, 69].

The most capable machines use some combination of active control and passive dynamics. Raibert's hopping and running robots were pioneering examples of this principle, using passive air springs and modulating the air pressure for powerful actuation [7]. In an effort to make better use of passive dynamics for improved efficiency, the ARL Monopod II used "Controlled Passive Dynamic Running" to achieve economic running dynamics with simple control laws [5, 70]. The Bow Leg Hopper uses a similar strategy, and one of these two robots most likely holds the record for world's most efficient running machine [40]. More recent hexapedal robots like RHex and iSprawl are the fastest and most robust running robots that exist today [71, 72]. The gaits have been described as "controlled flailing," relying on controllers and passive dynamics which have been refined through iteration.

It is an open question how much of the robot's behavior should be encoded in passive dynamics, and how much implemented through active control. The Actuator with Mechanically Adjustable Series Compliance (AMASC) was an attempt to place more of the passive dynamics in the mechanism by having physically variable compliance in the leg spring mechanism [73]. While the device functioned, it also highlighted several reasons that physically variable compliance has drawbacks that may outweigh the benefits for legged locomotion, making an argument for stiffness changes to be implemented in software rather than hardware.

Built on the lessons from the AMASC, Thumper [74] and MABEL use a non-

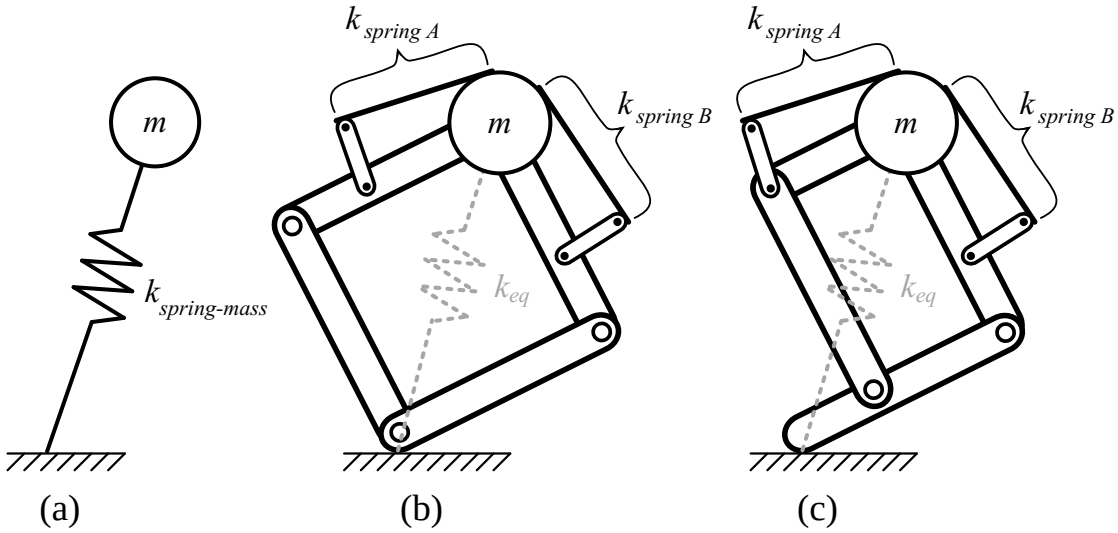

Figure 2.3: (a) The spring mass model, (b) Symmetric ATRIAS model, and (c) ATRIAS model. Note: the springs are plate springs (leaf springs).

adjustable physical spring, have successfully demonstrated 2D running gaits, and MABEL has demonstrated stable 2D rough-terrain walking. MABEL exhibits spring-mass-like behavior and has a mechanical cost of transport of only twice that of a human [75]. ATRIAS continues to build on the experience with MABEL, working towards robust, efficient locomotion in 3D, unsupported and untethered.

2.3 Robot Model

ATRIAS approaches the behavior of the spring-mass model through a four-bar linkage design shown in Figure 2.3. Both of the heavy leg motors are located at the hip, applying torques to series plate springs as shown in Figure 2.4.

The model for ATRIAS matches the dynamics of the spring-mass model in more

than a qualitative manner. We have shown that the dynamics are equivalent, with a mathematical proof in Appendix **??**. The proof describes forces acting only in the leg length direction, and no torques in the hip direction, and this is implemented on a real robot through a series-elastic force controller [76]. The spring deflections of actuators A and B are compared, and the motors adjust the deflections such that they are always equal to one another. Thus, the net torque about the hip joint will be zero, acting as a pin joint like the spring-mass model[3]. There are two practical differences between the ATRIAS model and the standard spring-mass model: first, the motors are coupled differently, such that adjusting either leg angle or length requires the coordination of both motors (Figure 2.4) rather than a single motor for each degree of freedom. Second, a linear spring about the leg joints of the ATRIAS model will lead to a nonlinear leg stiffness function which is dependent on leg configuration. It is unclear whether this is a benefit or a detriment. In practice, the springs can be shaped to implement any desired function, but the relationship between leg stiffness and length remains.

2.4 System Design

The defining characteristics of ATRIAS are the 4-bar leg, the plate springs, the motor placement and transmission design. In this section, we discuss those features and the reasons for them in detail. In addition, we explain details of the electronics

[3]The point mass m of the spring-mass model has no rotational inertia, $I = 0$. If one has a system with mass, m, with a non-zero rotational inertia, $I > 0$, one can approximate the spring-mass model with the use of a pin joint between the leg and the mass.

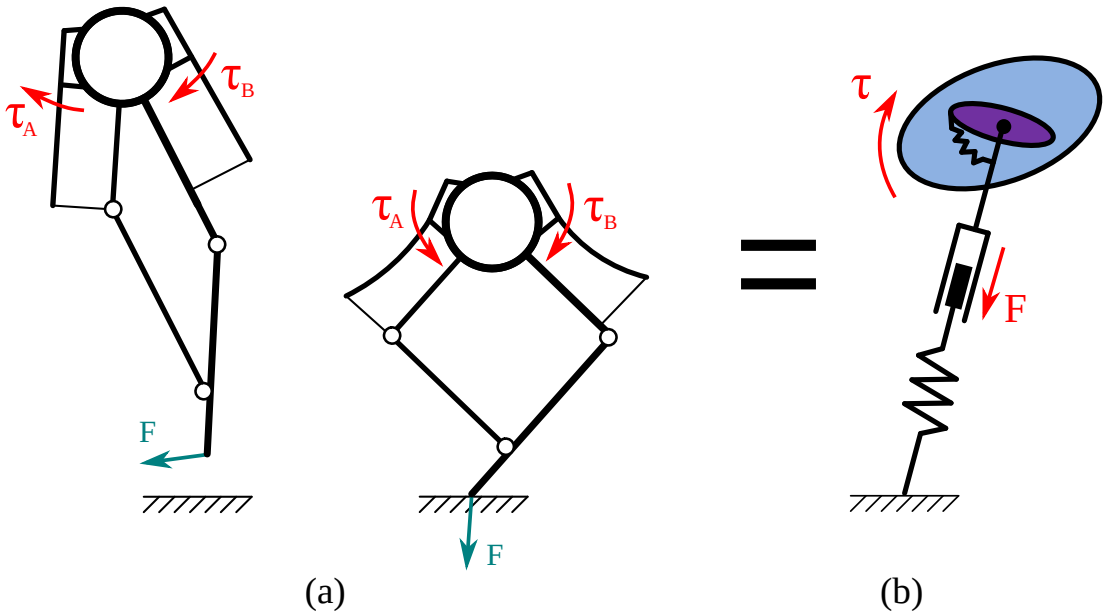

Figure 2.4: Coordinated movement of ATRIAS motors (a) can match movements of a typical actuated spring-mass model used in simulations (b).

and their placement on the machine, the support boom, and the hip joint and actuators.

2.4.1 Four-Bar Leg

The four-bar linkage for ATRIAS' leg is a clear example of bio-inspired design rather than biomimetic design, because it implements principles derived from the example of animal locomotion, interpreted via the spring-mass model, rather than replicating animal morphology. The four-bar leg clearly does not look like any animal leg, yet it approaches the massless "spring" half of the theoretical mass-spring system, and thus allows for regular ground impacts that do not lose much energy in

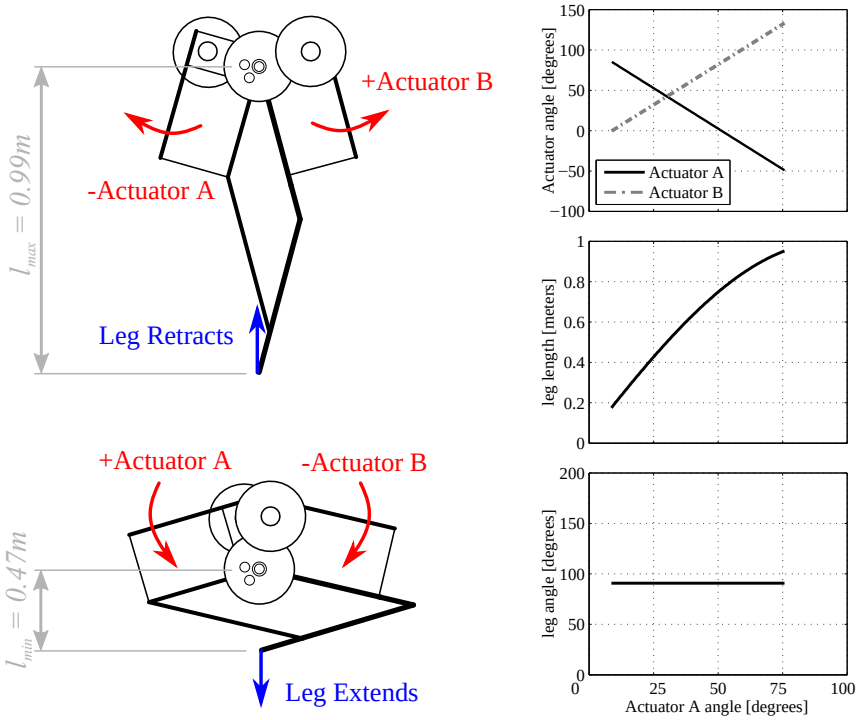

Figure 2.5: Actuator movements to accomplish leg retract and extend, $\pm(A - B)$. When the actuators rotate opposite directions the leg will only extend/retract (no change in leg angle).

the collision. When a robot is running, all components that must instantaneously change velocity at that ground impact are effectively part of the toe mass, and lead to inelastic collision energy losses and large force impulses. Linkages similar to the ATRIAS legs are used in high-speed pick-and-place robots, for the same reason–to reduce inertia, and allow high accelerations with low forces [77]. When compared to a prismatic joint, such as a standard pogo stick, the "effective inertia" of the leg, as measured by the impulse required to accelerate the toe from zero to some velocity, is much lower for the four-bar leg.

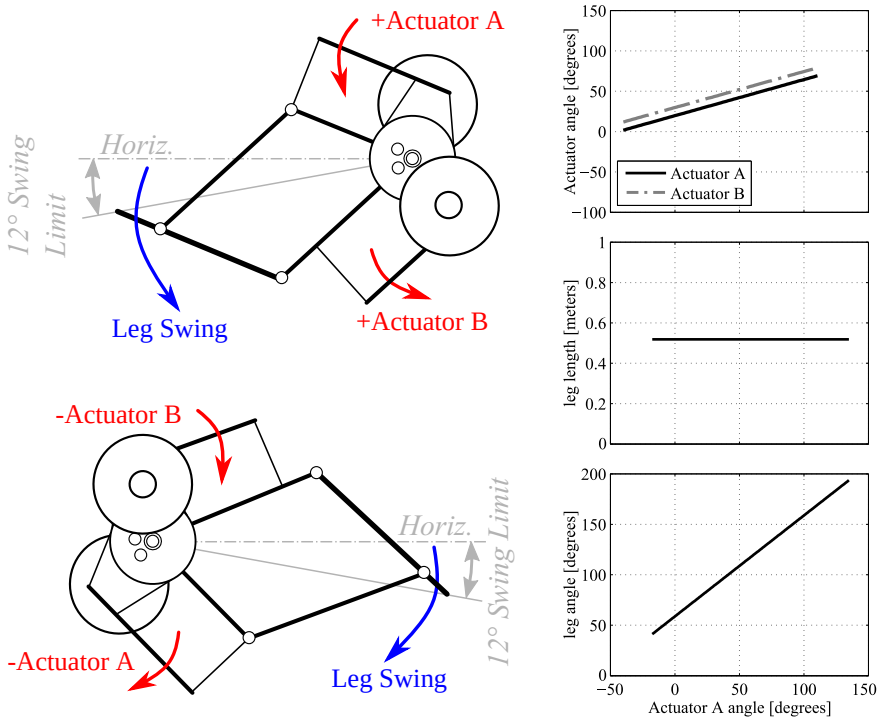

Figure 2.6: Actuator movements to accomplish leg swing, $\pm(A + B)$. When the actuators rotate the same direction the leg will only swing (no change in leg length).

The four-bar design allows both motors to coordinate their torques when extending the leg. This allows all of the motor power in the leg to be applied to leaping or hopping, as compared to relying on a single motor to lengthen or shorten the leg while the leg swing motor acts as dead weight. A literal spring-mass model relies on such decoupled actuation, as shown in Figures 2.5 and 2.6.

Springs are mounted in series with each motor and each link, as shown in Figure 2.8. Just as the motors must coordinate to extend the leg, the springs both influence the forces on the leg. If the motors are held stationary while ATRIAS is dropped vertically on the ground, the symmetry of the four-bar leg along with

identical springs generates a toe force that is vertical and passes through the center of mass, like the spring-mass model. Any asymmetry of the linkage, or in the spring stiffnesses, would modify this effect and cause the robot's passive dynamic behavior to diverge from the desired spring-mass behavior.

The four-bar leg has a number of engineering benefits that do not necessarily relate to the spring-mass model similarities. For example, when compared to a prismatic joint, rotational joints can more easily be made smaller, stronger, and lighter for the same load capacities. Wiring is much more convenient around rotational joints, for use with ground contact switches or other sensors on the leg. The four-bar legs allow for a large range of motion, from nearly straight to almost completely folded, as shown in Figure 2.5. Hard stops are implemented on all ranges of motion, including the range of each spring and the range of each link, with limit switches and dampers where appropriate to avoid damage to the robot. The limit of the spring deflection to its mechanical hard stop is shown in Figure 2.8.

One drawback of using knees is that, by fully extending the leg, a singularity is reached. For ATRIAS, a mechanical fuse is integrated into the two knees to safeguard the majority of components from damage in the event of a hard landing with an extended leg. This mechanical fuse is implemented as a set of nylon pins in the knee joints, which fail under relatively light loads. The knee is designed such that the lower leg will shear away from the upper leg, as shown in Figure 2.7.

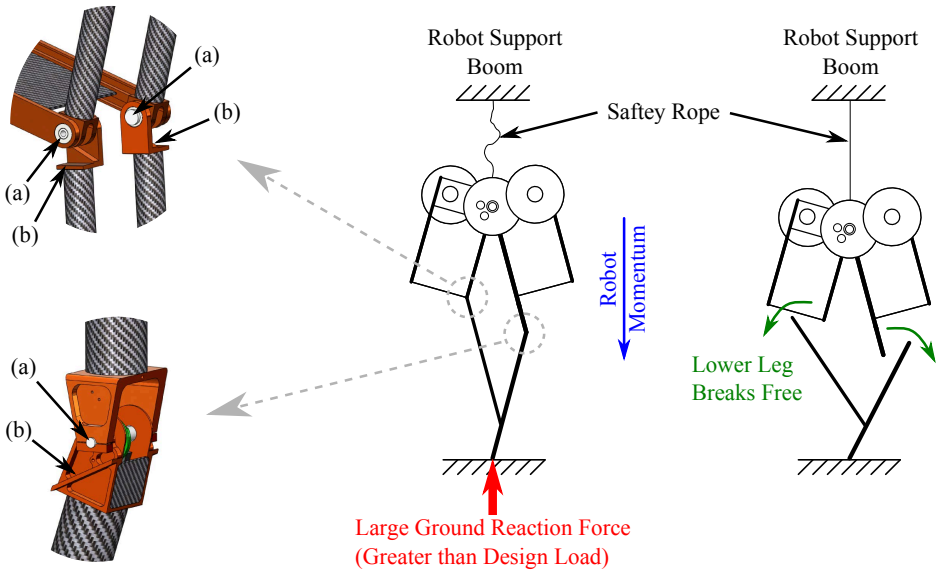

Figure 2.7: In the event the ground reaction force of the robot is greater than is safe for some of the more expensive components on the robot, the knee is designed to break away. Inexpensive nylon pins (a) are used as the mechanical fuse. The upper leg and the lower leg slide past each other along sloped surfaces (b) and are ejected away from the robot.

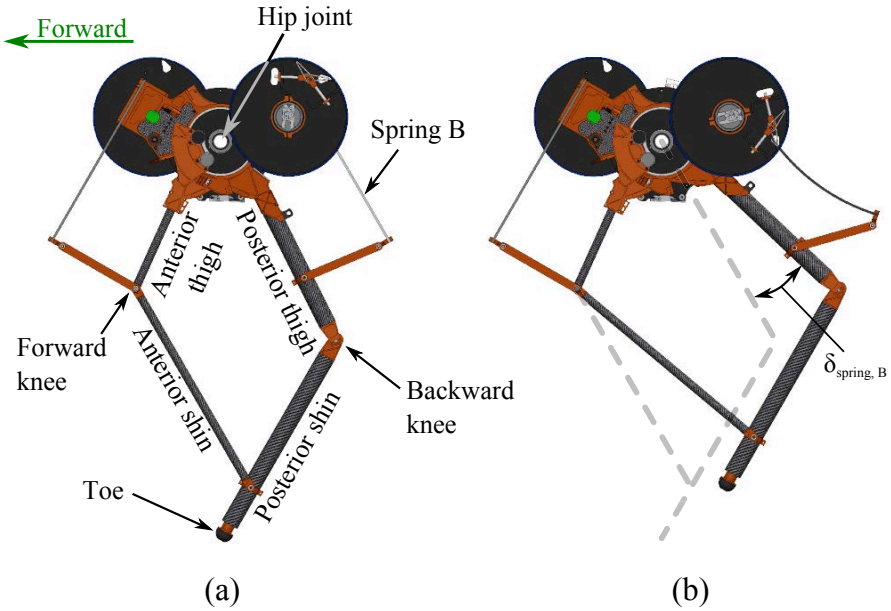

Figure 2.8: (a) Neutral springs (b) the series plate spring of Actuator B is flexed to the hardstop limit. $\delta_{spring,B}$ is measured by a 32-bit absolute encoder. Note: the motor of Actuators A & B and the spring of A have not moved.

2.4.2 Plate Springs

The springs used in ATRIAS are flat plates made from unidirectional fiberglass composite, the same material used in compound archery bows. This material has higher energy density than steel springs, has low internal damping, is more stable over humidity, temperature changes, or aging than polymer springs, and is convenient to fabricate. While the spring material demonstrates near-linear spring behavior, the four-bar linkage imparts a mechanical advantage that generates a softening spring function in the leg length direction. It is unclear what spring function is desirable for the legs; the spring-mass model uses a linear spring primarily for mathematical convenience. As theory or experimental results suggest

different desired spring functions, the plate springs can be shaped to approximate any desired spring function. They are convenient to replace in between experiments, so different stiffnesses and stiffness functions can be directly compared in experiments on ATRIAS.

The spring stiffness is chosen such that the natural frequency of the robot mass and the leg spring matches the stride frequency of a target running gait. However, in flight, the low inertia of the leg in series with the leg spring results in high amplitude free vibrations of the leg. While this does not have a strong influence on the robot dynamics, it is an aesthetic consideration, and could lead to problems with sensing.

2.4.3 Motors

Frameless, brushless motors were chosen for the highest torque density for a given mass budget (custom-wound MF0210 series from Allied Motion), and the transmission and leg were designed around their flat, large diameter shape. As discussed earlier, the four-bar leg allows the motors to coordinate their power for leaping motions, and their location at the hip joint helps locate the center of mass in a spring-mass-like location. Although the motors are efficient and provide adequate torque, they introduce an unavoidable rotational inertia that is not represented in the spring-mass model, and is large enough that it cannot be safely ignored.

When the leg lengthens or shortens, the motors rotate in opposite directions, as shown in Figure 2.5, and their reaction torques exactly cancel one another. When

swinging the leg forward or backward, both motors rotate in the same direction as the leg, Figure 2.6, and their combined rotational inertia is large enough to cause the body to pitch significantly in the opposite direction. This effect can be mitigated either by adding significant body inertia, or using a reaction inertia such as a tail or a second leg; for bipeds, the two legs can have approximately equal and opposite accelerations, thus reducing the reaction torques of the motors. In hardware testing experiments with ATRIAS, the problem was addressed by constraining body pitch rotation with the support boom.

The concept of coordinating the two motors to extend the leg length via the four-bar linkage has clear advantages in terms of applying peak leg forces, and at least one important drawback: for running and walking gaits, there is an internal power expense that does not contribute energy to locomotion caused by geometric work, as defined by [78], where one motor drives the other. Shown in Figure 2.9a, both motors apply a holding torque to allow the series springs to absorb and release kinetic energy from the gait, accelerating the body back upward to the end of stance phase. Concurrently, the robot is rotating the leg backward as it moves the body forward over the toe during a running or walking gait. As a result, both motors are rotating in the same direction while applying torque in opposite directions. Thus, one motor is producing positive power, while the other produces negative power.

$$\begin{aligned} p_1 &= \tau_1 \cdot \dot{x}_{leg} > 0 \\ p_2 &= \tau_2 \cdot \dot{x}_{leg} < 0 \end{aligned}$$

Considering the robot as a blackbox system, Figure 2.9b, an external observer would calculate the total power generated by the robot and output on the world would be similar to that calculated from the spring-mass model. In fact this observed power, $p_{black\,box}$, would be based on the difference in motor torques. This difference is non-zero because τ_1 must be greater than τ_2 to cause leg swing during stance).

$$p_{black\,box} = \tau_{leg} \cdot \dot{x}_{leg} = (\tau_1 - \tau_2) \cdot \dot{x}_{leg}$$

This is larger than the actual power output by the system which is the sum of the absolute power output from each motor, p_{leg}.

$$p_{leg} = p_1 + |p_2| = \tau_1 \cdot \dot{x}_{leg} + |\tau_2 \cdot \dot{x}_{leg}|$$

Thus, the overhead of the internal power expense requires motors of higher power capacity than necessary for the gait, considering the black-box system observations. Some energy may be recovered through regenerative effects within the negative power motor, however, this is reduced by inefficiencies such as mechanical transmissions and electrical power electronics. It remains to be seen whether the benefits of sharing torque outweigh the drawback of an internal power overhead; the tradeoffs differ depending on the goals of the gait, and will be discovered in practical experimentation. For example, strictly vertical hopping or leaping would benefit from the ATRIAS leg configuration, allowing load sharing between the leg motors, while a fast walk might unnecessarily waste energy due to the geometric work.

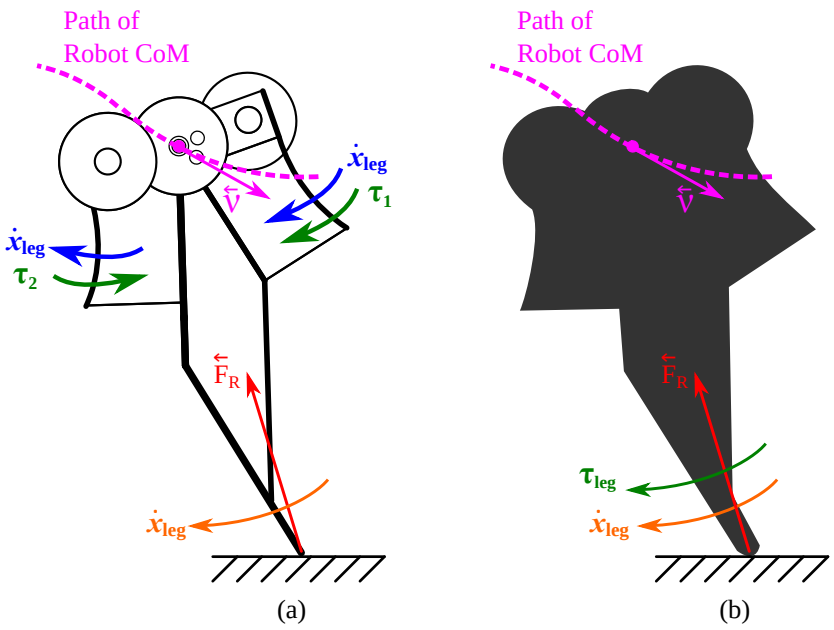

Figure 2.9: The ATRIAS motor configuration with the four-bar linkage leg costs more power, due to geometric work, and requires that the motors be sized with greater power capacity that one would initially consider. This drawback may outweigh the benefit of torque sharing of the motors for high power leg extension tasks such as leaping or running. Observing the robot as a black box system, case (b), the power output by the leg is observed to be $p_{black\,box} = \tau_{leg} \cdot \dot{x}_{leg}$. Alternatively for the robot, the actual power is the sum of the absolute power output by both motors within the leg, case (a), which is $p_{leg} = \tau_1 \cdot \dot{x}_{leg} + |\tau_2 \cdot \dot{x}_{leg}|$, which is greater than $p_{black\,box}$. The difference in these two observed power values is the internal power overhead, caused by geometric work.

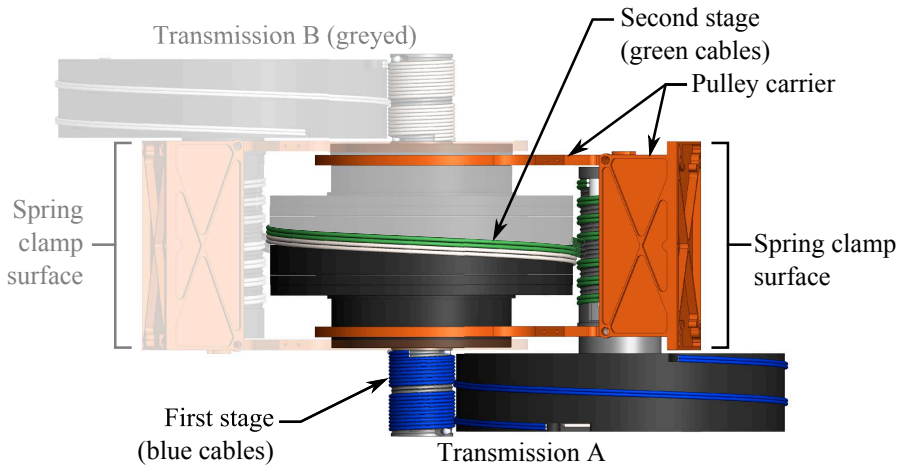

Figure 2.10: Top down view of both Epicyclic Cable Drive transmissions on ATRIAS 1.0 (other components of robot removed for clarity). Notice the large pulley in the second stage of each transmission (the motor housings) is common to both.

2.4.4 Motor Transmission

The transmission developed for ATRIAS is, to our knowledge, the first of its kind: a compound epicyclic, or planetary, cable drive. As a cable drive, there are many features that are ideal for legged machines, such as zero backlash, high torque transmission, low mass, and high mechanical efficiency. In ATRIAS, there are two motors, and two identical transmissions incorporated into the leg; both are seen in Figure 2.10. Each section of the transmission is symmetrical, and designed to work together with its copy located on the opposite side of the motors. The motors are placed back-to-back, with the motor shaft serving as the "sun" of the planetary cable drive, extending out of the motor housing on both sides. The large diameter section of the planet pulleys engages with the motor shaft, and

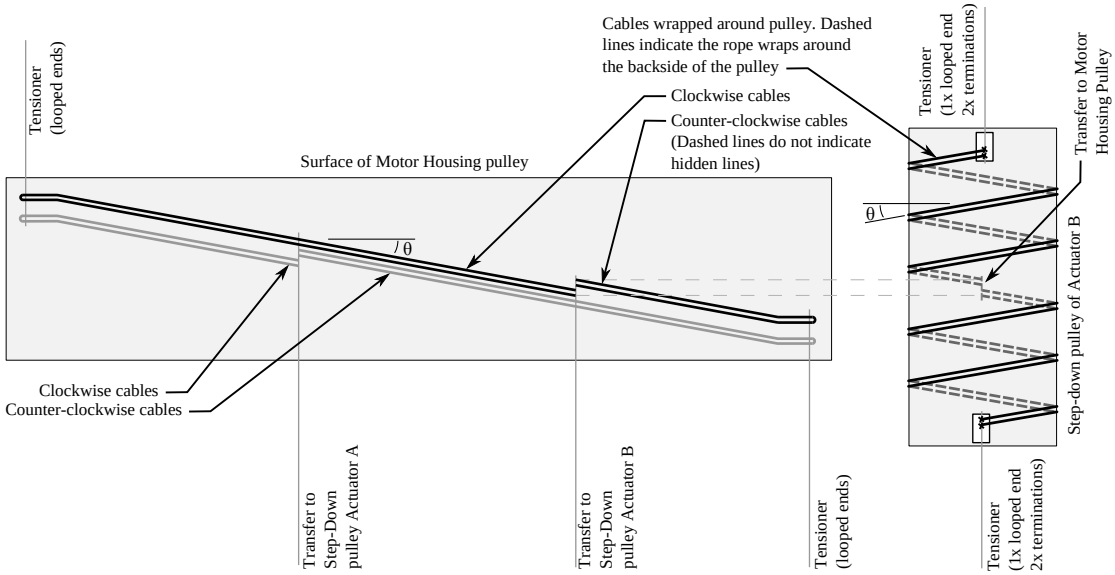

Figure 2.11: Flat pattern schematic of the second stage pulleys of both Compound Epicyclic Cable Drive transmissions. Note that the cable pitch, θ, is constant between mating pulleys, despite their difference in diameters.

the small diameter section of the planet pulleys engages with the motor housing, which serves the same purpose as an outer ring gear in traditional planetary gear transmissions. The planet pulleys are mounted in a carrier, shown in Figure 2.10, and schematically in Figures 2.12, and 2.13. As the motor drives the planet pulley, it rolls around the housing of the motor, driving the carrier, which is mounted to the base of the springs, which then drives the four-bar leg.

The cables apply torque via terminations on each pulley, as shown in Figures 2.14, 2.16 and 2.15; they do not rely on friction to transmit torque. As such, the pulleys have a limited range of motion, and cannot rotate indefinitely. The range of motion of each degree of freedom of the ATRIAS leg is 152.5 degrees, and with a transmission ratio of 20:1, the motor pulley must rotate approximately 8.5 times.

As such, the cables must wrap in a helical manner around the pulley to avoid overlapping. Two cables are necessary, wrapping in opposite directions, to apply torques in both the positive and negative directions. The pitch of the cables is determined by the smaller pulley diameter and the width of the cables, as shown in Figure 2.11. The axial length of a pulley is determined by the desired rotational range of motion and the pitch angle of the cable wrapped around the pulleys, or, $l_{pulley} = (pitch) \cdot (number\,of\,revolutions)$ where the *pitch* is the inches of axial travel (length) of a cable per revolution. Added to this length, l_{pulley}, is the cable wrapping in the opposite direction, and additional length for cable terminations.

The helical wrap of the cable is enforced by a set of round grooves in the *small pulley* only. Grooves can only be made in only one pulley of a pair, because grooves in both pulleys can lead to cable pinching and interference with very slight mismatches caused by changes in pre-tensioning or cable stretch. The grooves are in the smaller pulley rather than the larger one because the greater curvature of the smaller diameter leads to larger forces flattening the cable, and thus a groove to support the cable's round cross-sectional shape is more important. On the large pulley, because the cables are wrapped around a much larger radius, the cable tension applies relatively little force in the flattening direction. As recommended by cable manufacturers, the grooves are round, sized 5-10% larger than the nominal cable diameter, and support the cable under $\frac{1}{3}$ of its circumference [79]. This shape is a balance between supporting the cable's round shape under load, increasing the surface of contact between the cable and pulley to minimize wear on the cable or pulley, and avoiding friction and wear from rubbing, which would occur if the

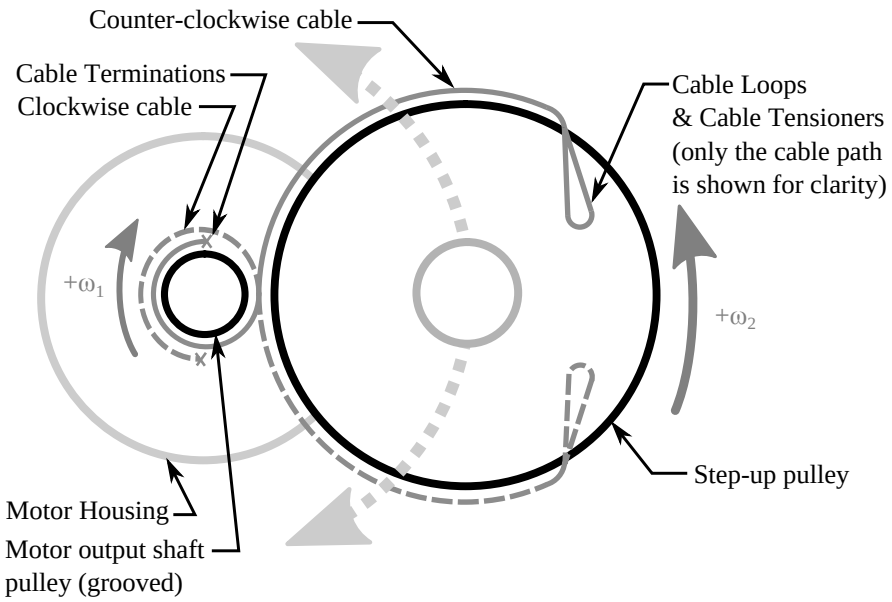

Figure 2.12: Schematic view of First Stage of Epicyclic Cable Drive transmission. The large step-up pulley rotates around the smaller motor output shaft pulley, driving the second stage of the transmission. The large step-up pulley here is clamped to the small step-down pulley in the second stage. Each tension member (solid and dashed grey) are single lengths of stainless steel cables looped back on themselves yielding two tension members. Not shown is the pulley carrier that constrains the step-up and step-down pulleys to rotate around the motor housing and motor shaft

grooves were very deep.

Cable drive transmissions can become rather large when they are designed to handle the significant torque seen in ATRIAS, and when a large transmission ratio is required. The torque capacity is determined by the working load of the cable and the diameter of the smallest pulley; but the pulley size is limited to a minimum of 20 times the diameter of the cable to maximize cable life[4] [79]. For example, a 1/8"

[4]20:1 is nominal for maximizing life. 15:1 can be used for shorter planned life spans or low cycling frequency designs.

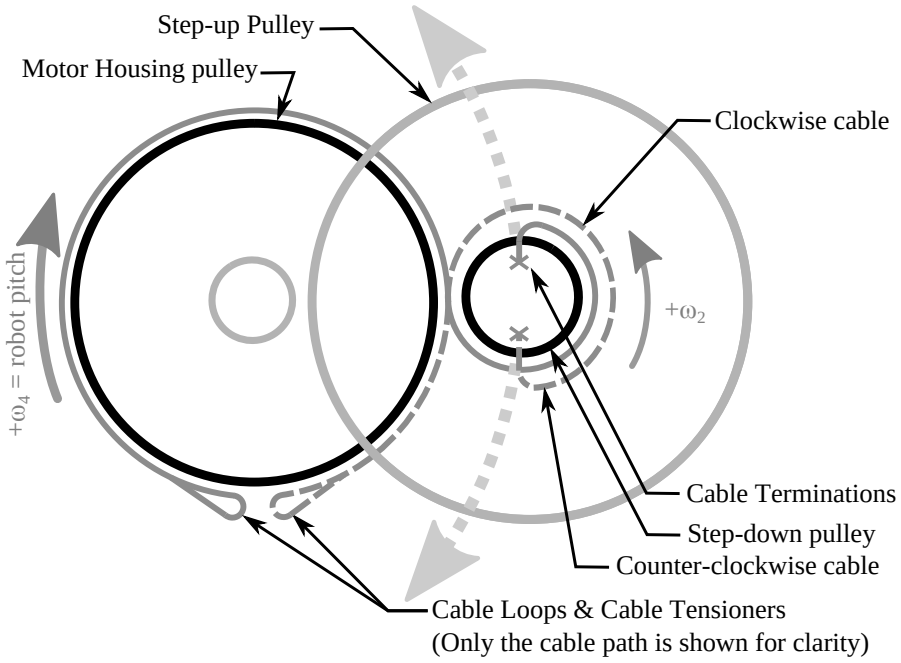

Figure 2.13: Schematic view of Second Stage of Epicyclic Cable Drive transmission. The large pulley is the motor housing and the smaller rotates around the larger, moving one end of the plate spring. The Small step-down pulley is clamped to the large step-up pulley in the first stage of the transmission. Each tension member (solid and dashed grey) are single lengths of Vectran rope looped back on themselves yielding two tension members. Not shown is the pulley carrier that constrains the step-up and step-down pulleys to rotate around the motor housing and motor shaft

cable wrapped around a 2.5" diameter pulley that is bolted to the motor shaft, and assuming a working load of 20% of the breaking strength (798kg for cable 2126 at [79]), the pulley and cable can handle about 50Nm of torque. With a 3.74:1 ratio, the larger pulley will be 9.35" in diameter, and have a torque capacity of 186Nm. The motor can output a theoretical peak torque of 56Nm applied directly to the smaller pulley while the larger pulley will experience a peak applied torque of 209Nm from the motor, greater than the working capacity of either pulley. Torque capacity of the pulleys can be increased by using multiple strands of cable in parallel, as we have done in both stages of the ATRIAS transmission. With two cables the pulley will have torque capacities of 100Nm for the smaller and 371Nm for the larger giving a safety factor of about 1.5. These are the design values for ATRIAS 1.0 and are the result of iteration of these calculations to reduce the size of the large pulley. The parallel strands are part of a single cable, with loops at an end, so cable tension can be exactly balanced between the multiple strands. This approach avoids the problem of individual strands having slightly different lengths, which would result in unequal sharing of the load.

The cable terminations and tensioning mechanisms for ATRIAS are shown in Figures 2.16 and 2.15. Both use a screw mechanism to tighten cables, and both are a loop of cable rather than a cable end. The cable ends are terminated in a fixed feature of the small pulleys, as shown in Figure 2.14. Figure 2.11 shows the cable path in a flat pattern schematic view; both ends of the cable begins at a termination on the small pulley, and the pair of strands wrap around the pulley in the helical grooves until they transition to the large pulley, and continue to

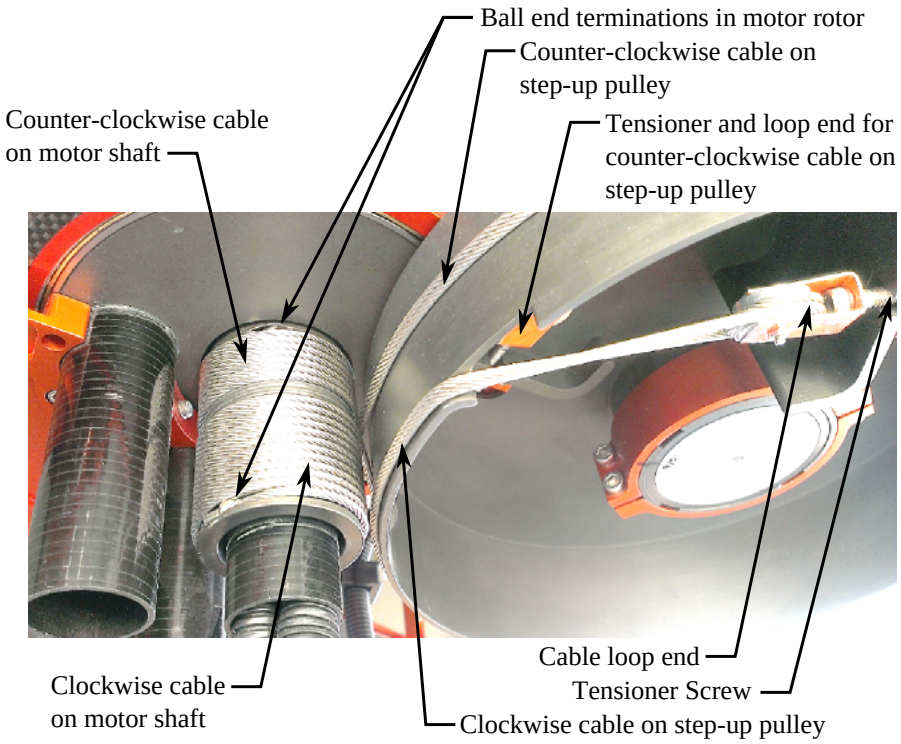

Figure 2.14: Detail close up of the steel cable terminations, winding and tensioning systems in the first stage of the transmission.

wrap around the large pulley until they reach the tensioner. At the tensioner, the cable loops around a cylinder that is no less than 5x the cable diameter; this can be small because the cable will not repeatedly wrap or unwrap around this cylinder, and thus limited plastic deformation is acceptable. The entire path of the cable must be smooth and circular, avoiding any sharp bends or kinks as these cause stress concentrations, weakening the cables. The same approach for cable terminations and tensioning can be used with four strands or more, as needed to decrease the small pulley and cable diameters, and/or increase the load rating of the transmission.

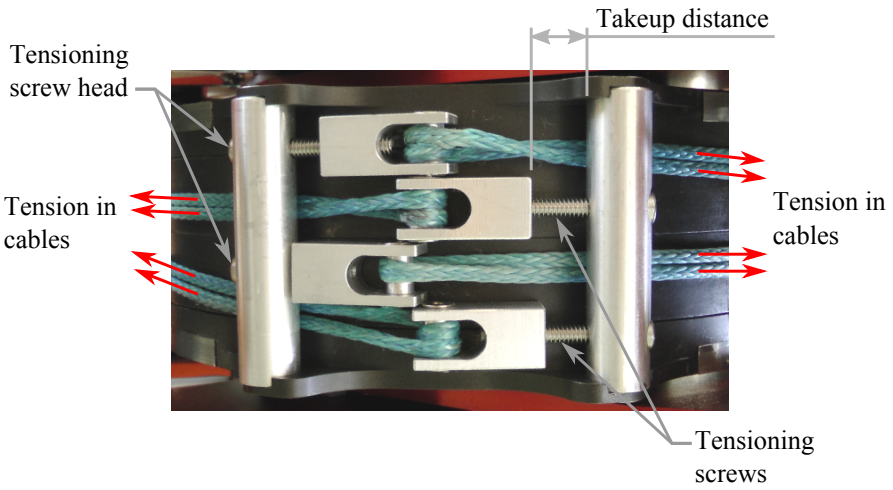

Figure 2.15: The cable tensioner for the second stage of the transmission is at the base of the motor housings shown here consisting of a pair of opposing tensioners for both the A and B actuators. Tension in the cables is increased or decreased by turning the appropriate screw.

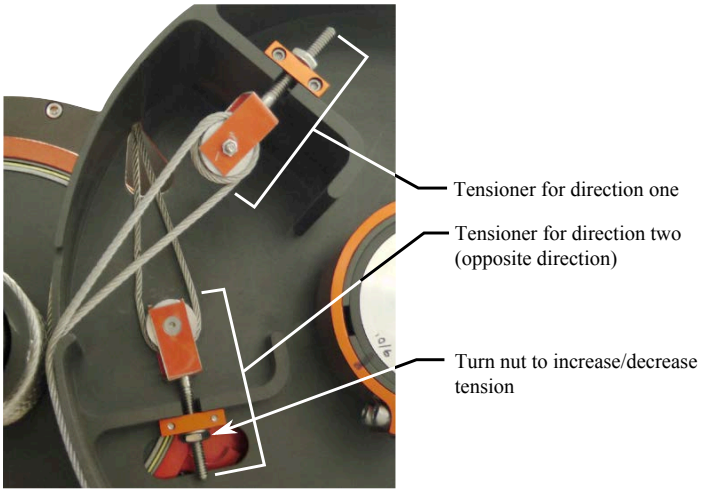

Figure 2.16: The cable tensioner system for the first stage of the transmission is contained within the large pulley consisting of one tensioner for each direction of cable. Tension is adjusted by turning the nut.

Cable drives to date have generally been implemented with finely stranded stainless steel cables wrapping around hard-anodized aluminum pulleys, and this is the approach for most of ATRIAS as well [74, 80–82]. Stainless steel is a good material for cable drives, and easy to purchase from a variety of sources; however, other materials are more suitable in some situations. Based on an informal study [83], Vectran and Tungsten are promising. Tungsten is more durable than steel, although much more expensive. Vectran is stronger and lighter, but is limited to slow speeds to avoid melting. We speculate that internal friction or damping causes this issue. Other polymer materials suffer from destruction due to internal abrasion (Aramid), extreme photosensitivity (Xylon), low stiffness (Spectra), and creep (all polymer materials but Vectran and Xylon) [79, 84] . For our application, where cable tension must be maintained over the life of the machine, even small amounts of creep are not acceptable. Vectran seemed worth exploring as an alternative to stainless steel, and is used in the second stage of the ATRIAS planetary cable drive, shown in Figure 2.15. The speed is adequately slow to avoid melting, the strength of the Vectran is higher than steel, and this is our first experiment in using Vectran for a cable drive application.

We encountered some challenges using Vectran that were not initially considered with steel cable. First, Vectran requires different methods for cable terminations. While steel cables can have brass or steel crimps swaged onto the ends (ball end, threaded, etc.), and made-to-order cables with terminations can be purchased, Vectran is terminated using a spliced end loop, as shown in Figure 2.17. Knots cannot be used, as they will cause stress concentrations and reduce the load

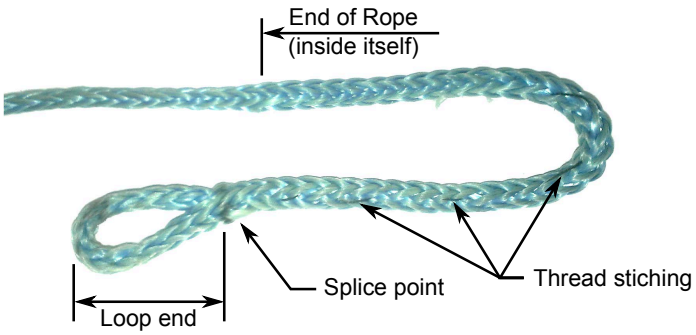

Figure 2.17: Spliced end of Vectran rope. The rope is looped around the termination and inserted back into itself for several centimeters, about 6 inches for the $\frac{1}{4}$ inch diameter rope pictured here. When the rope is under tension the end, interior rope, is held in place from compressive pressure of the exterior rope as it is stretched to it's working length and diameter.

capacity of the rope. Other methods, such as an epoxy plug on the end of the cable, are plausible but were not tested on ATRIAS. A second challenge related to the braided construction: after initially tensioning the rope, working it around a pulley will cause the braid to relax somewhat. After several times re-tensioning the cable, the tensioning mechanism sometimes reaches the extent of its limited length. With sufficiently long cable tensioners, a few stretch-and-work cycles will bring the rope to a stable tension.

In testing ATRIAS with the Vectran, it functioned well and did not wear out during the life of the robot experiments. The Vectran is less abrasive than steel, and thus does less damage to aluminum pulleys when under high load. Vectran is worth considering for low-speed, high-force cable drive designs.

The ATRIAS compound planetary cable drive meets the goals of high efficiency and high torque with zero backlash. However, it is physically very large, leading

to excess weight and packaging challenges. Figures 2.5 and 2.6 show the 152.5° range of motion for leg swing, and as the leg swings, the planet pulley follows through the range of motion, sweeping out a large "keep away" area for any other robot body or leg components. For this reason it is difficult to find an area for attachment of the motors to a robot body. In future designs, this will be a careful consideration. For a smaller range of motion, or for a single degree of freedom, or a lesser transmission ratio, the configuration would be excellent.

2.4.5 Additional Systems

The defining features of ATRIAS, such as the transmission and the four-bar leg, are the primary contribution of the machine and of this paper. However, they constitute only half of a robot. The following sections discuss the hip actuators, electronics, sensing, and support boom which enable ATRIAS to function.

2.4.5.1 Hip Adduction and Abduction (Lateral Actuation)

While the spring-mass model is a planar construct, ATRIAS is a prototype for a 3D bipedal machine, which requires hip adduction and abduction. Further, as the ATRIAS prototype is mounted to a boom (desribed later in this paper), adduction and abduction will be required to accommodate the kinematic constraints imposed by the boom when the robot is in a contact with the ground. The initial design of the ATRIAS lateral actuator is shown in Figure 2.18 and 2.19. The pivot point is

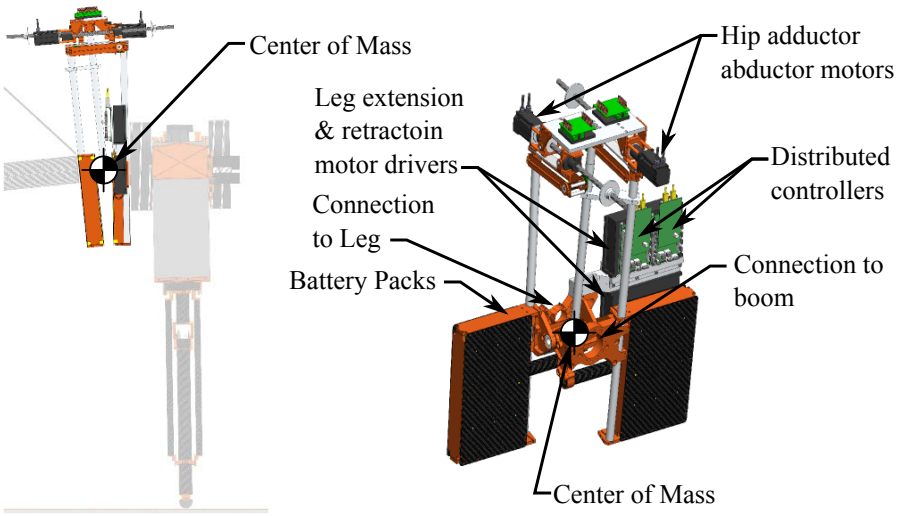

Figure 2.18: The adductor and abductor actuators of ATRIAS with electronics and motor drivers located. The center of mass of this assembly is placed at the hip axis to maintain center of mass location of the complete robot to the spring-mass model.

at the center of mass, intersecting with the planar leg swing DOF. Long lever arms allow for a backlash-free torque increase and speed reduction. A series elastic actuator is created using a small fiberglass leaf spring and a ball screw driven by a brushless motor, with an absolute magnetic encoder for spring deflection measurement. The purpose of this approach is to control forces on the leg during running gaits; in the lateral direction, we anticipate that the normal approach will be to apply zero force during stance phase to act as a pin joint, relieve stresses caused by the kinematic constraint with the boom [85], and during flight phase to place the leg appropriately for the gait policy (for example equilibrium gait refer to [9]) . Further, control of the lateral leg force is a convenient method for addressing the kinematic constraints of hopping while connected to a boom.

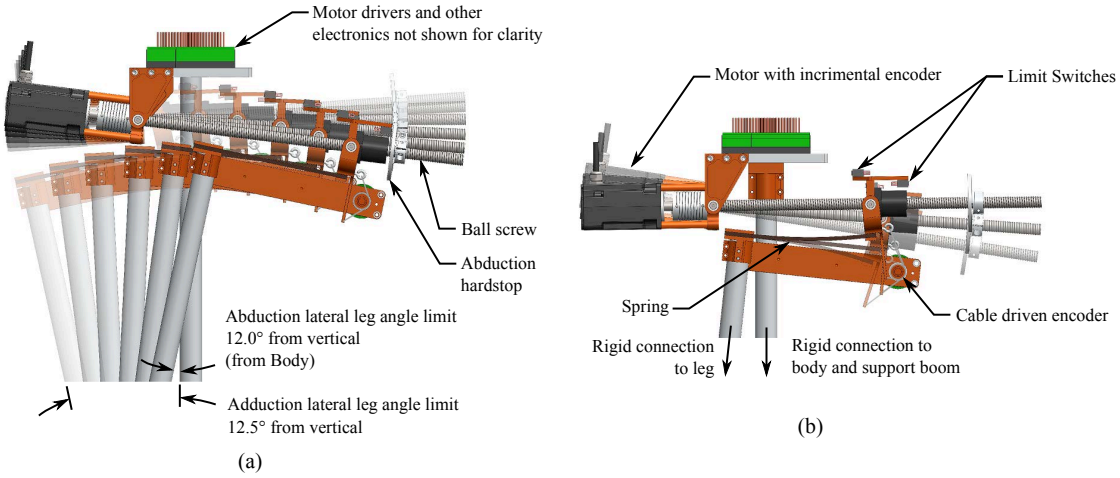

Figure 2.19: Detail view of lateral actuator. (a) range of motion of the actuator. (b) deflections in the spring measured by an absolute encoder with cable pulley. An absolute encoder is placed on the hip joint axis (not shown). One of these actuators would be attached between each leg and the body of a biped configuration. Inclusion of a series spring allows for sensing and control of the lateral forces and stresses in the leg.

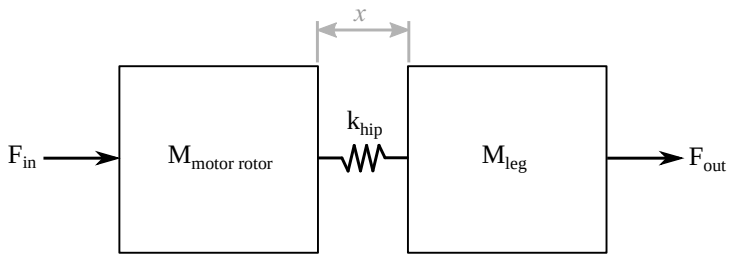

Figure 2.20: Simple rigid body dynamical system diagram of the lateral leg angle actuator for ATRIAS 1.0 monopod. The compliance of the hip adduction and abducting actuator, k_{hip}, makes controlling x with little or no overshoot difficult. This figure is a linear representation of a rotational system for simplicity.

Upon completion, a fatal flaw in the design became apparent. The leg has significant mass, and as such, it bounced significantly on the series spring of the lateral actuator and made control difficult. The spring and force sensing should not have been placed between the load mass (the leg motors) and the lateral actuator motor inertia. Shown in Figure 2.20, we can see that this design results in a mass-spring-mass system with only a single actuator, making control of desired forces difficult. In practice, the lateral actuators did not perform as desired, and the spring was essentially locked out for experiments with the robot. We instead relied on position control and flexibility in the leg to overcome the kinematic constraints of the boom, and future designs will use force control and spring stiffness closer to the end effector to avoid the mass-spring-mass problem.

Table 2.1: List of Sensors used on ATRIAS 1.0

What is sensed on robot	Type of Sensor	Manf./Supplier
Motor rotor (transmissive encoder)	2,800 Lines/Rev. incremental quadrature	US Digital
Motor rotor (hall effect)	3 sensors (1 per phase)	Emoteq
Motor winding thermal switch	Switch, resistance $\propto$ temperature	Digikey
Motor output after transmission	13-bit absolute (766μRad/bit)	Renishaw
Four-bar link - 'forward thigh'	32-bit absolute (25.6μRad/bit)	Renishaw Resolute
Four-bar link - 'backward thigh'	32-bit absolute (25.6μRad/bit)	Renishaw Resolute
Ground contact with toe	SPST momentary NC	Digikey
Range of motion limit switches	SPST momentary NC	Digikey
Robot pitch (boom sensor)	17-bit absolute (geared 12.6μRad/bit)	Hengstler
Robot horizontal (boom sensor)	17-bit absolute (geared 107.3μm/bit)	Hengstler
Robot vertical (boom sensor)	17-bit absolute (geared 26.8μm/bit)	Hengstler

2.4.5.2 Sensing

The sensors on ATRIAS are designed to provide full state information for the robot, with the highest resolution possible, at a 1kHz update rate. There are a number of magnetic and optical encoders to provide proprioceptive information about every degree of freedom, and with very high resolution position measurements, velocities and accelerations can be calculated well. In addition to position encoders, a momentary switch is included at the toe such that ATRIAS can determine whether it is in contact with the ground or not, useful for determining which state the robot is in (aerial or stance phases). Finally, limit switches on each hard stop will allow the machine to shut down in case of a control error. Our list of sensors is included in Table 2.1, and the complete electrical and software architecture design is outlined and described in [86].

2.4.5.3 On-Board Electronics and Body Design

While including all systems necessary on board for the robot to operate untethered, careful attention was given to the placement of electronics on ATRIAS 1.0 to place the center of mass at the hip joint, following the requirement set forth by the goal of matching dynamics with the spring-mass model. To accomplish this, batteries and power electronics are placed symmetrically around and slightly below the hip joint offsetting the mass of the lateral actuator, electronics and computer placed high above the hip. This makes up the body of ATRIAS 1.0. A potential danger in this design is that the components are not protected in the event of a unconstrained fall. In a future version of ATRIAS these components would be relocated or protected in some way to prevent damage that might be incurred during a fall.

2.4.5.4 Robot Support Boom

A support boom was constructed to support the lateral degrees of freedom (DoF) of the robot while allowing free motion forward-backward, up-down, and pitch, as well as sensing of these DoFs. Supporting the robot in this fashion is useful in the final stages of engineering and early in the development of planar controllers, before considering controllers for 3D locomotion. The boom is 2.10 meters in radius and constrains the robot to a circular path fitting snugly within our lab. The boom provides sensor feedback in the form of rotary encoders, Table 2.1, measuring the robot's position in the lab. This is in place of, and preparation for, an inertial measurement unit (IMU) mounted directly to the robot body.

To prevent the robot from crashing into the ground, a catching rope is attached between the robot end of the boom to a rotating lifting eye attached to the ceiling in the lab. The catch rope length is set such that if the robot were to fall, the rope would go taught before the knee of the robot touches the ground. The knee is chosen because it is the furthest reaching part of the robot that can incur major damage if subjected to an impact with the ground. This is true with the condition that the thigh is perpendicular to the ground, otherwise the compliance of the plate springs will help in preventing damage to other components above the knee.

Other planarizing robot support systems described in [85] were considered in place of the boom but were ultimately rejected in favor of a lower added inertia to the robot, and on the basis that future tests with ATRIAS will involve forceplates and obstacles. Treadmills can not easily incorporate forceplates (for comparison to bio-mechanic data and insight as to how the robot is interacting with the world), or obstacles such as stairs, ramps, drop steps, or non-rigid ground (compliant and/or damping). However, a treadmill can be added to the boom later if necessary.

It is observed with this iteration of the boom that stiffness of structural members has a strong influence on sensor measurements. The booms' sensors are located at the gimbal, at the other end of the carbon tube from the robot. Carbon fiber tubing is ideally suited as the long structural member between the gimbal and the robot due to its high stiffness and low mass, adding little inertia to the robot. However, the 1.5 inch diameter tube used in this first design iteration has insufficient stiffness, allowing high amplitude, low frequency oscillations that are easily visible. These oscillations influenced the boom sensors, giving an inaccu-

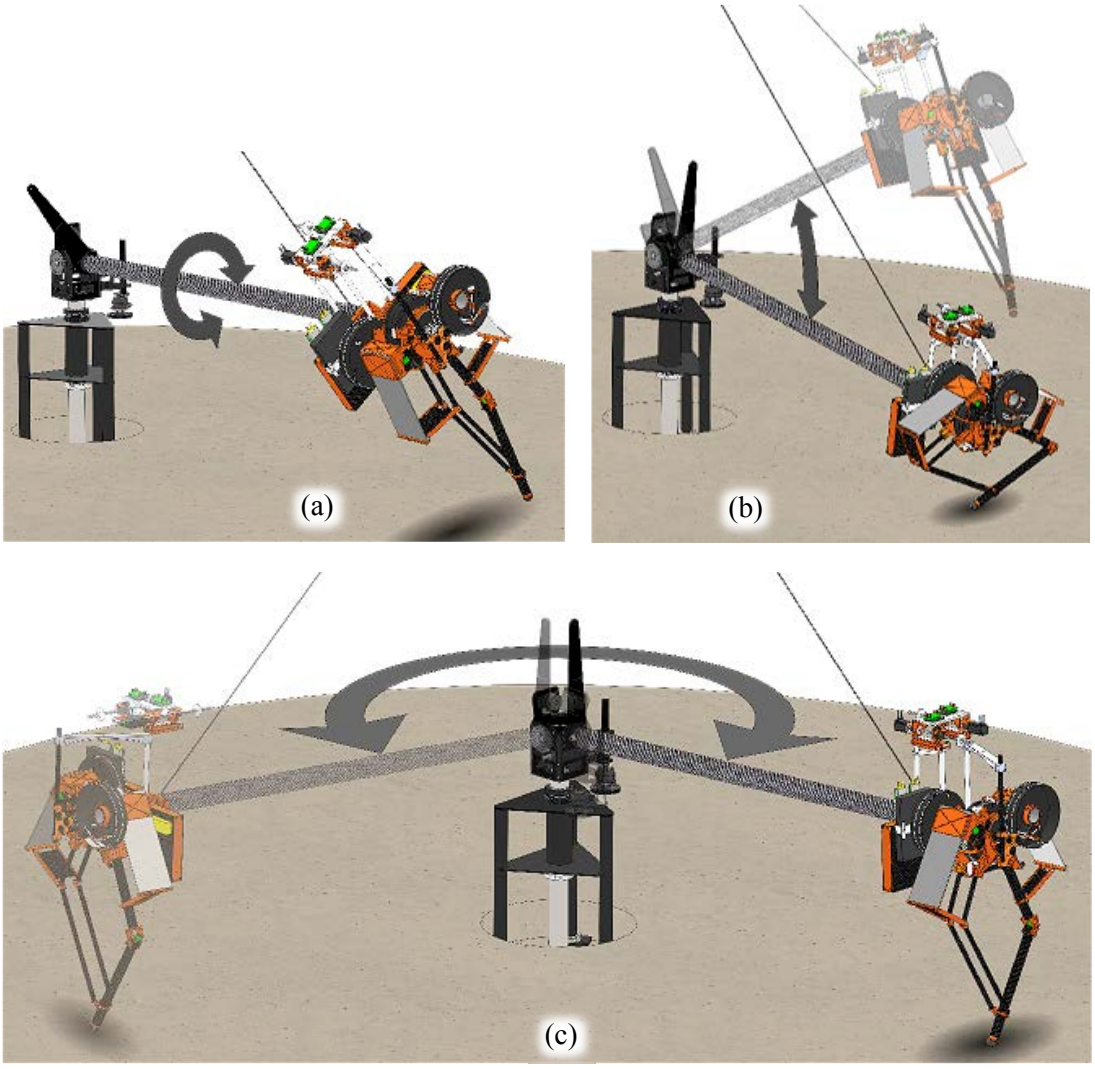

Figure 2.21: Robot support boom (a) robot pitch DoF, (b) vertical DoF, (c) horizontal DoF, each of which is sensed by a 17-bit absolute encoder to allow the robot to compute it's position relative to the ground.

rate measurement of the robot's position and velocity, leading to instability in gait controllers.

The boom is a useful platform to test the prototype ATRIAS 1.0 in preparation of building a biped ATRIAS, capable of untethered 3D locomotion. Like ATRIAS, it will undergo some design revisions to address problems with stiffness and sensing resolution. The basic design is sound, influences the robot dynamics minimally because of very low moving mass, provides good sensor feedback, and prevents physical damage from falls.

2.5 Conclusion

ATRIAS 1.0 is an example of model-based robot design, and we suggest that this approach will lead to more successful dynamic robots. ATRIAS successfully maintained a stable hopping gait with spring-mass-like behavior, as shown in Figure 2.2. The symmetrical design of the four-bar leg with series plate springs and motors placed at the hip joint axis allowed for an analytical match between the dynamics of ATRIAS and the spring-mass model, and will allow for controller development on the simple model to be implemented directly on the robot.

The compound epicyclic cable drive transmission is a novel mechanism that offers the benefits of zero backlash, high torque transmission, low mass and high mechanical efficiency. It is very effective for limited range of motion, as in a legged machine. The primary drawback to this transmission is size; the large keep-out volume swept by the pulleys as the orbit around the motor housing is larger than

anticipated during early design stages. Further, the transmission was somewhat wide due to the helical wrap of the pulleys. A smaller range of motion would require less cable wraps and a narrower transmission. The size of the transmission and keep-out volume made connection to the hips difficult, as the keep-out volume swept most of the diameter of the motor housings. These packaging issues are much more apparent after building a prototype, and can be addressed early in the design stages for future machines.

Vectran rope appears to be a good material for use in slow-speed cable drives, assuming the termination and tensioning accommodates the material appropriately. Lubricating the Vectran and steel cables reduces internal friction and significantly extends the life of the cables as well as making it easier to work tension along the length of the Vectran cable around the pulleys.

When designing actuators with series elasticity, it is critical to consider the location of the load mass, and the capacity for the motor and spring to handle that load mass. The large leg springs and primary motors work well, because the leg mass is light is easily handled by the leg springs; but the hip abduction/adduction motor performed poorly and demonstrated significant uncontrolled oscillation, because the series spring was between the rotor inertia and a large load mass that included the primary leg motors.

Series compliance paired with the low inertia four-bar leg demonstrated free vibration during the unloaded aerial phase of the gait. This behavior must be accounted for when implementing controllers that make decisions based on spring deflection.

The fiberglass plate springs work very well as a series spring providing large momentary energy storage and near perfect energy recovery. These springs exhibit a linear force deflection relation that paired with the four-bar leg behave as a softening spring. It is not known what spring behavior is best for a particular gait at this time, but the advantage of ATRIAS as a research platform is that it can exhibit a variety of leg stiffness behaviours through the use of force control methods. Different plate springs can be easily interchanged to explore the the effect of different spring rates for a set of locomotion goals.

The four-bar leg does serve to minimize leg inertia, does allow load sharing of the two motors when applying force in the leg length direction, and does implement spring-mass behavior well–however, the power expense of the geometric work is a major concern. This feature is sufficiently important that minimizing or eliminating the power overhead may be a constraint for leg configuration designs in future robots.

The implementation of a mechanical fuse at the knee served to protect more expensive and difficult to replace components and was in fact useful. After many hops, it was discovered that the plastic pins in the knee joint had significantly deformed. This indicates that the design load was reached and perhaps exceeded yet the fuse did not work. A key point for this feature is to use a sufficiently brittle material whereas a tougher material will not break away completely and elude detection.

Arrangement of the on-board electronics was such that the center of mass was at the hip joint and the sagittal plane. While this is a direct match of the spring-mass

model it may be impractical for future robots with a torso, manipulators, sensor packages, or otherwise of humanoid form. The center of mass may necessarily not be at this location and thus drive research to explore this extension of the spring-mass model into bipedal robotics. Protection of these components necessary for tether free operation from damage during a fall or other hazardous interactions with the environment is a serious consideration for future prototype and finished robots.

While not the focus of this mechanical design paper, ATRIAS 1.0 is the first implementation and test of a high level controller with distributed control at a high rate (1kHz). This is accomplished with off the shelf Advanced Motion Control motor drivers, a medium power nettop computer running a real-time Linux operating system with open source software including Robot Operating System. Further details and an in-depth discussion can be found in [86].

Supporting this early prototype and catching it in the event of a fall, the robot support boom proved a valuable tool. Sensing of the robots position in the world is provided by sensors on the boom in place of a future inertial measurement unit necessary for tether free operation. Stiffness in the boom structure lacked in this version and will be increased in future versions but must remain low mass as to minimally add to the robots inertia.

This paper describes ATRIAS, an example of a model-based robot. The machine demonstrated spring-mass behavior, successfully achieving the goal of generating passive dynamics that match a simple, controllable reduced-order model. It is our hope that this paper will lead to further development of these ideas and

continued improvement of walking and running robots.

Acknowledgments

Thanks to Jonathan Luc, Devin Koepl, Kevin Kemper, and Alex Sheehan, of the Dynamic Robotics Laboratory at Oregon State University for their hard work in building and operating ATRIAS 1.0. Thanks to Michael Summers for his work conducting a study of the pros and cons of various steel cables and polymer rope on anodized aluminum pulleys for use in a cable drive. Thanks to Siavash Rezazadeh for help error checking the ATRIAS to spring-mass model analytical equivalency proof. Thanks to Professor Ross Hatton for helping us hone the story of this paper. Thanks to Ross Hatton and Andrew Peekema for help reviewing this paper prior to submission.

Supported by Human Frontier Science Program (HFSP) grant number RGY0062/2010.

Appendix

The appendix of this paper is moved to the appendix of the Thesis in order to follow formatting guidelines of the University. Please see Appendix A

Chapter 3 – ATRIAS 2.1: Enabling Agile Biped Locomotion with a Template-Driven Approach to Robot Design

Practical bipedal robots need to be simultaneously efficient, robust, and versatile machines, but designing robots dynamically capable of these demands has been a significant bottleneck. We designed ATRIAS to be a highly dynamic biped capable of both walking and running untethered in real environments. To meet this goal, ATRIAS is designed to approximate a dynamically capable locomotion template, *i.e.* the *spring-mass model*. We identify the challenges of this template-driven design approach and present our solutions to make ATRIAS a real-world-viable human-scale machine. We show that ATRIAS exhibits behaviors predicted by spring-mass models in fulfillment of our design approach. Particularly, ATRIAS reproduces the characteristic ground-reaction forces of human walking and running, a key dynamical feature of spring-mass locomotion. We also demonstrate ATRIAS' capacity to walk, hop on one leg, bound like a spring-mass hopper, and recover from an unseen plunge into a 6.5-inch-deep gravel pit. Further, by building efficient spring-mass dynamics into the mechanical system, ATRIAS, when pushed, walks several steps without its actuators replenishing lost mechanical energy. These combined hardware experiments validate

ATRIAS' capability as a platform for spring-mass robot controllers and for agile and economical locomotion in general.

3.1 Introduction

Bipedal robots face a daunting set of locomotion challenges, making them a tough topic for mechanical design. To be useful, robots must be sufficiently economical to complete their journey, robust to damaging falls, and exhibit enough versatility in gaits and motions to cope with varied environments. To date, most legged robots (and bipeds in particular) have failed to meet these demands simultaneously, either being too energy-guzzling or motion-specialized to make the leap into application. We posit that such robots are held back by inherent dynamical limits which are imposed by their mechanical design.

ATRIAS 2.1 is a human-scale bipedal robot (Figure **??**) constructed with the primary goal of having the dynamical capabilities necessary to freely traverse the varied environments of the human world. As such, designing ATRIAS' mechanics to enable, not encumber, the locomotion dynamics is a paramount consideration. To ensure dynamical capability, we adopt a *template-driven* design approach. This means that ATRIAS (**A**ssume **T**he **R**obot **I**s **A** **S**phere) is mechanically designed to maximally embody the dynamics of a target model, an uncommon design philosophy among human-scale robots. By approximating a dynamical model theoretically capable of variety of agile and efficient gaits, we can expect ATRIAS to be similarly capable in kind.

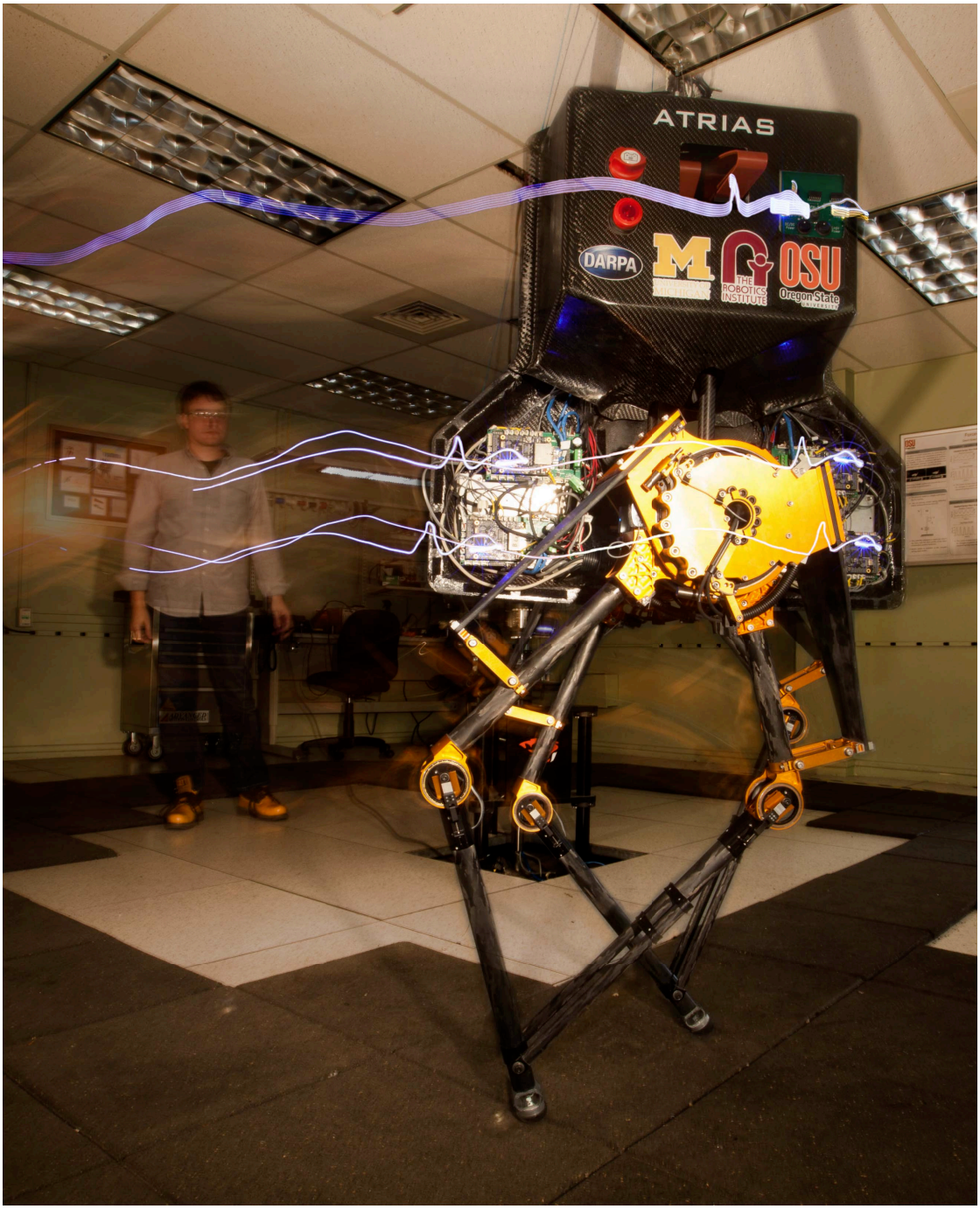

Figure 3.1: Long exposure photograph of ATRIAS performing a spring-mass walking gait as described in Section (insert reference here).

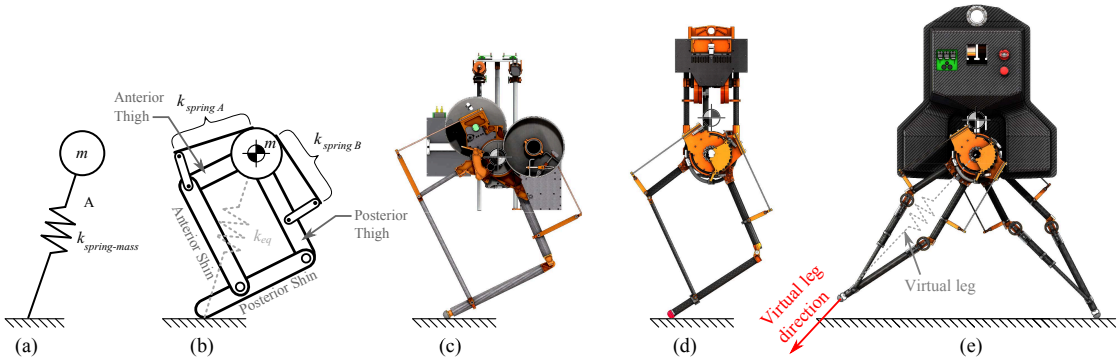

Figure 3.2: The design evolution of ATRIAS from simple model to single-legged prototype to full biped. (a) spring-mass model for legged locomotion (b) ATRIAS model with naming convention of the four-bar linkage members (c) ATRIAS 1.0 prototype monopod (d) ATRIAS 2.0 prototype monopod (e) ATRIAS 2.1 biped with virtual leg direction indicated as a line that intersects the toe and he hip joint axis

ATRIAS' template-driven design approximates key features of the *spring-mass model* (Figure 3.2a). The spring-mass model produces versatile locomotion, having been suggested as a unifying framework across walking and running gaits [87, 88], as well as gaits for quadrupeds and hexapods [89]. It is a generally well-studied template [90–96], which has spurred an abundance of specialized spring-mass control techniques. Their implementation on ATRIAS would make it an established anchor for template based control strategies in the real world.

Here, we highlight the key mechanical design features of ATRIAS 2.1, experimentally demonstrate ATRIAS' capacity to be a versatile and economical machine through its embrace of spring-mass dynamics, and argue the merits of template-driven design for practical robots.

For background, Section 3.2 catalogs the successes and limitations of bipedal

robots and template-driven robot designs to date, and describes the spring-mass model (ATRIAS' target template). Section 3.3 outlines the design features which were key to approximating the spring-mass model, their design impact, and our solutions to constructing a pragmatic, template-driven biped. Section 3.4 reports a number of hardware experiments which validate that ATRIAS functions as a spring-mass robot, including its ability walk . We further demonstrate the capacity of ATRIAS 2.1, and its monopedal predecessor ATRIAS 2.0, to execute a variety of dynamic maneuvers: walking with human-like ground-reaction forces, hopping on one leg, bounding, and reflexively recovering from a hop into an unexpected 6.5-inch-deep gravel pit. In summary, Section **??**, we take inventory of ATRIAS' capabilities and assess template-driven robot design as an approach to enabling agile legged robots that are ready for the real world.

3.2 Background

While the concept of legged locomotion is inspired by nature, the engineered systems, especially in bipedal robotics, often did not exceed the stage of morphological biomimetics. The challenges of keeping balance, managing the dynamic interaction with the environment and adapting trajectories according to terrain changes are addressed in a number of ways.

In varying combinations, preexisting bipedal robots have exhibited versatile behaviors, been off-tether capable, tackled the challenge of human-scale implementation, and even approximated a dynamical template, but ATRIAS 2.1 is the

first robot to combine all of the above. Aside from few hybrids, two general approaches are taken in designing bipedal walking machines, namely fully actuated humanoids and minimally actuated template-driven machines.

3.2.1 Fully-Actuated Humanoids

Fully articulated humanoid robots have been the most practical and publicly visible representatives of bipedal locomotion. Notable examples such as Honda's ASIMO [97], AIST's HRP series [98], KAIST's HUBO [99] are electromechanically driven, fully actuated machines capable of versatile, autonomous motion carrying their energy source. These high-DOF robots address the challenge of bipedal balance by careful regulation of their zero-moment point (ZMP) [100]. However, ensuring controllability of the ZMP calls for actuators and stiff mechanical connections at every joint. This systematic rigidity prevents these humanoids from exhibiting bouncy, highly dynamic locomotion. This full actuation approach also consumes a lot of power, exhausting on-board batteries in impractically short time spans (estimated under 30 minutes) and sporting energy transport costs an order of magnitude greater than their human counterparts [101].

3.2.2 Template-Driven Robots

Another class of bipedal robots locomotes with only little or no actuation utilizing the passive dynamics of the mechanical system. While exhibiting very efficient

locomotion, their action is limited to few gaits and very specific environmental conditions. This class comprises of so called passive dynamic walkers [101], the design of which was driven by the inverted pendulum model for walking [66], and their motorized offspring.

Few robots incorporated compliance to enhance dynamic capabilities alongside energy efficiency. They show more or less versatile behavior and a large range of gaits. Among them the Raibert hoppers [102], the ARL monopod [103], the CMU bowleg [104], the template driven Jena Fox [105] as well as Mabel [106], a precursor of ATRIAS.

3.2.3 Spring-mass model: dynamics and control

The spring mass model has been proposed originally as a template for running and hopping [87]. It has been used to model and explain animal locomotion by reducing the system complexity while preserving the general dynamics [19,107,108]. The use of highly reductionist models to describe dynamical systems for legged locomotion on land and to investigate control strategies was formalised by [109].

One of the advantageous features of the spring-mass-models is its passive dynamic stability [110]. Stability analysis has been combined with the template model to test hypothesis of neuromechanical functions [111]. The use of stability as an objective function for control gave rise to a number of control strategies to respond to various pertubations during locomotion [90–96]. The same model has also been found to be able to produce bipedal gaits [88], reproducing a number of features of

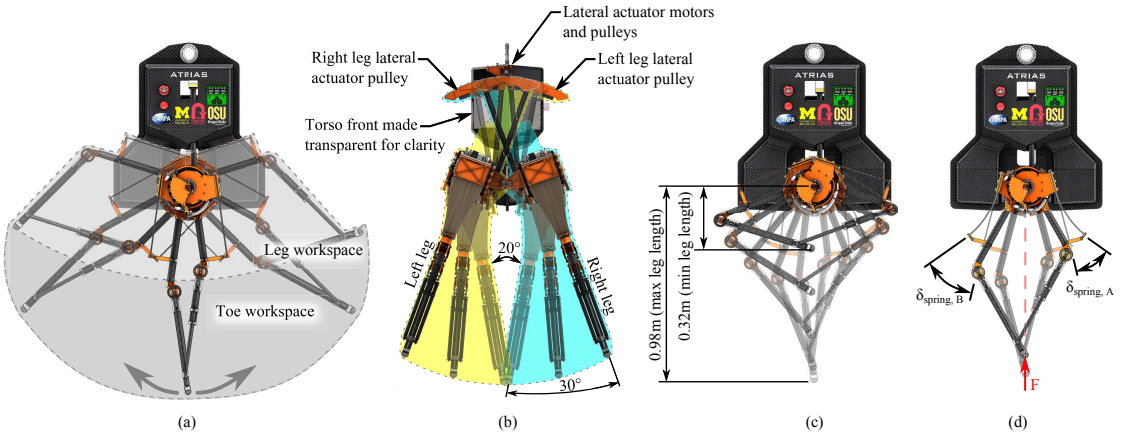

Figure 3.3: Workspace of the leg in the (a) frontal plane and (b) sagittal plane and (c) the range of motion for leg length and (d) the maximum kinematic spring deflection.

animal walking [112], and could be extended towards control strategies for trunk stabilisation [113].

Spring-mass locomotion is also maximally efficient, sporting a theoretical energy cost of zero which has spurred an abundance of specialized spring-mass control techniques which could be plausibly employed on ATRIAS [9,114]. For biologists, spring-mass dynamics serve as dynamical predictors of animal locomotion, modeling organisms from cockroaches [115], to lizards [109], to humans [87], to quail [116], making ATRIAS a potential platform for biological investigations.

3.3 System Design

Rendering ATRIAS into both a template-driven and practical robot requires meeting two sets of specifications: 1) approximating key *template features* and 2) recon-

ciling practical *robot design realities*. Approximating template features facilitates the dynamic behavior we require, while "design realities" ensure that robot states are measured, components are protected and housed accessibly, and the robot can maneuver outside the sagittal plane (the typical domain of the spring-mass model).

3.3.1 Implementation of Template Features

Equipping ATRIAS with the dynamical advantages of the spring-mass model entails approximating four of its key mechanical features: 1) a massless leg, 2) the remaining robot mass centered near the hip joint, 3) mechanical compliance between the ground contact and hip joint, and 4) restricting leg forces to the virtual leg axis. These template features are primarily achieved through ATRIAS' leg mechanism, a two-degree-of-freedom series-elastic leg (Figure 3.2b).

3.3.1.1 Massless Leg

To approximate the massless leg of the spring-mass model, we designed ATRIAS' leg mechanism to be a lightweight fourbar linkage (schematic illustrated in Figure 3.2b). The linkage has two degrees of freedom, allowing for a large range of motion for the toe in the sagittal plane, as drawn in Figure 3.3a. The four-bar linkage is constructed of lightweight and stiff carbon fiber with aluminum joints, yielding less than 4% of the robot mass that inelastically impacts the ground with every

step[1].

3.3.1.2 Hip-Centered Body Mass

with the two proximal links (anterior/posterior thigh) independently actuated via a series-elastic motor.

3.3.1.3 Series Compliance

Series compliance on ATRIAS is achieved with use of plate spring made from fiberglass bar stock. Fiberglass is chosen because of its high coefficient of restitution, and stable spring stiffness with temperature, ageing, and humidity changes. The springs themselves exhibit a linear spring behaviour while the four-bar leg combined with springs exhibits a softening spring behavior; with decreasing leg length the mechanical advantage of the four-bar decreases, increasing the torque on the springs.

3.3.1.4 Axial Leg Forces

All leg forces in the spring-mass model are exclusively axial, with no tangential forces inducing net moments about the hip joint. The parallelogram mechanism configuration further ensures that equivalent torques on the proximal links create

[1]The components of each leg distal to the series plate springs weighs 2.4 kg, compared to a 62 kg robot mass. For most gaits, only one leg impacts per step.

resultant forces along the virtual leg axis.

3.3.2 Robot Realities

While essential template properties are matched with the above features, there is a necessary set of requirements for the robot to function, untethered and unsupported, in the real world. These include sensing and measuring forces, the software and electrical system, actuation, and component housing and protection.

3.3.2.1 Measuring Forces

Deflections of each fiberglass plate spring is measured by a set of two high resolution absolute encoders giving very accurate force measurements allowing for good force control with the leg. Force exerted by the spring is the product of the spring coefficient, k, the deflection in the spring, δ, measured by absolute encoders with 294 µrad/Bit, one at the base of the spring the other at the cantilevered end, Table 3.1. This measurement paired with the kinematics of the leg yields the axial force interaction between the ground and the toe allowing for this force to be controlled with the motors. The value for k is measured with an external device prior to the installation of the spring to the robot.

While the spring deflection measuring sensors are of a high resolution and can measure the axial force applied to the leg, it is not useful to use these sensors to detect ground contact. The springyness of the leg paired with it's low inertia cre-

ates free-vibration during flight phase that one could confuse as a ground reaction force. Instead this is measured with a strain gauge at the toe.

3.3.2.2 Actuation

Two of the three leg motors work together to swing and shape the leg in the sagittal plane. These two motors each drive one of the anterior and posterior thigh members through a series plate spring. Movement can be coordinated to achieve changes in leg length or leg angle, Figure 3.3 (a) and (c). Proximal placement of these motors reduces the leg inertia as well as the moving mass. Additionally, the two motors work together to extend the leg, adding torques, useful for high power tasks such as running or jumping.

Gearing of the two leg motors is achieved with a compact harmonic drive. This change from the first prototype of ATRIAS (version 1.0 featuring a cable drive transmission) is made to reduce the keep-out zone around each leg, giving more room around the hip joint to connect each leg to the body. Both harmonic drive and cable drive feature zero-backlash, high torque capacity. The harmonic drive is more compact, reducing workspace requirements.

The third and final motor for each leg drives the leg laterally, or in the frontal plane, extending the planar leg into a 3-dimensional workspace, Figure 3.3b. The motor is placed high up in the torso and drives a pulley segment on a large lever arm giving a 56:1 gear ratio. A timing belt is used between the pulleys for the benefits of high force capacity, ease of assembly, zero-backlash.

3.3.2.3 Feet, in absentia

Unlike many of its robotic counterparts, ATRIAS has no actuated feet, nor "feet" of any sort. Its legs terminate with simple hooves. This makes standing still nontrivial as "point feet" have no effective polygon of support. Further, the spring-mass model supports only axial leg forces, and therefore has no control authority to regulate body position while standing.

So with these impediments in mind, why not include feet? In short, we don't have a firm understanding of how feet will impact ATRIAS' desired gait dynamics, perhaps jeopardizing the driving motivation of ATRIAS' design. For example, expanding the surface area of the foot will yield a larger support polygon, but affects the rotational dynamics during walking and running. Also, an overly heavy foot exacerbates ground impacts, eroding energy economy and exciting inconvenient oscillations in the series-elastic actuators.

We weighed the consequences of including feet and considering approaches to foot design, and ultimately, we deemed feet unnecessary to achieve ATRIAS' goals. Two design approaches were considered, a passive foot mechanism and an actively controlled foot actuator. For a foot to satisfy ATRIAS' dynamical goals and have utility on the robot, it would need to be 1) useful for balancing and 2) minimally impact the gait dynamics. An actively controlled foot would apply regulating torques while standing and zero torque during locomotion. Such an actuated design would likely add nontrivial mass to a leg designed to be lightweight. A passive foot could be made comparatively lightweight, but would have the same

underlying dynamics for standing, walking, and running. This was likely to result in a foot joint either too rigid to run or too compliant to stand.

Further, ATRIAS' inability to statically balance is not a crippling design flaw. While the spring-mass model does not have the proper actuation to balance without taking recovery steps, ATRIAS does, as it can apply tangential forces at the toe to actively regulate the body state. Further, more dynamic approaches to stability are available for legged robots, such as taking a step to recover (i.e. capture points [117]). At this juncture, we argue that building feet is a complex solution to an otherwise manageable problem.

3.3.2.4 Software and Electronics Specifications

The integration of electronics and software was driven by the design requirement to combine commercial hardware and open-source software. Sensor processing and motor control is fascilitated by a number of microcontroller-enabled (ATmega128, Atmel, San Jose, CA, USA) electronic stacks that are connected via ETHERCAT-bus to a commercial computer (Mini ITX, i1000A, OEM Production, San Francisco, CA, USA). The control system runs at 1000 Hz on a real-time linux kernel and was developed using Robot Operating System (ROS) and the Orocos framework. A detailed description of the control system design is available in [86]. Each motor and the associated sensors, among them 32-bit linear encoders (RL32BAT, Renishaw, Wotton-under-Edge, UK), limit switches and thermal sensors (Tab. 3.1), is controlled by one electronic stack, placed in the body (see Sec. 3.3.2.5).

Table 3.1: List of Sensors used on ATRIAS 2.1

What is sensed on robot	Type of Sensor	Manufacturer/Supplier
Motor rotor (transmissive encoder)	2,800 Lines/Rev. incremental quadrature	US Digital
Motor rotor (hall effect)	3 sensors (1 per phase)	Emoteq
Motor winding thermistor	temperature	Digikey
Transmission Output(s) (spring base)	32-bit absolute (294μRad/bit)	Renishaw Resolute
Four-bar link - 'anterior thigh' (spring end)	32-bit absolute (294μRad/bit)	Renishaw Resolute
Four-bar link - 'posterior thigh' (spring end)	32-bit absolute (294μRad/bit)	Renishaw Resolute
Toe in contact with ground	Strain gauge	Omega
Range of motion limit switches	SPST momentary NC	Digikey
Robot pitch (boom sensor)	17-bit absolute (geared to 12.6μRad/bit)	Hengstler
Robot horizontal (boom sensor)	17-bit absolute (geared to 107.3μm/bit)	Hengstler
Robot vertical (boom sensor)	17-bit absolute (geared to 26.8μm/bit)	Hengstler

3.3.2.5 Component Housing and Protecting

Protection of all internal components for robot falls is achieved with a shell-like design of the body structure made from composites. The body is composed of two halves, a stiff and strong structure made from carbon fiber with balsa core with fiberglass inserts for mounting points, Figure 3.4a, and a lightweight cover made from carbon fiber with no core. The resulting shell is strong enough to resist damage from a fall during a running gait, protecting components from impact damage and wires from snagging. The components are bolted to the structural half of the body and are accessible when the cover half is removed. The top of the body features a lifting eye for use with the existing robot support boom or an overhead gantry system for catching the robot during fall to prevent it from smashing into the ground.

In the event of large lateral forces on the leg beyond the design limit the knee allows for a controlled break of the leg by way of a mechanical fuse. The four-bar leg is inherently strong in plane and lacking stiffness out of plane. Use of nylon pins and screws allow the lower limbs, anterior and posterior shins, to break away

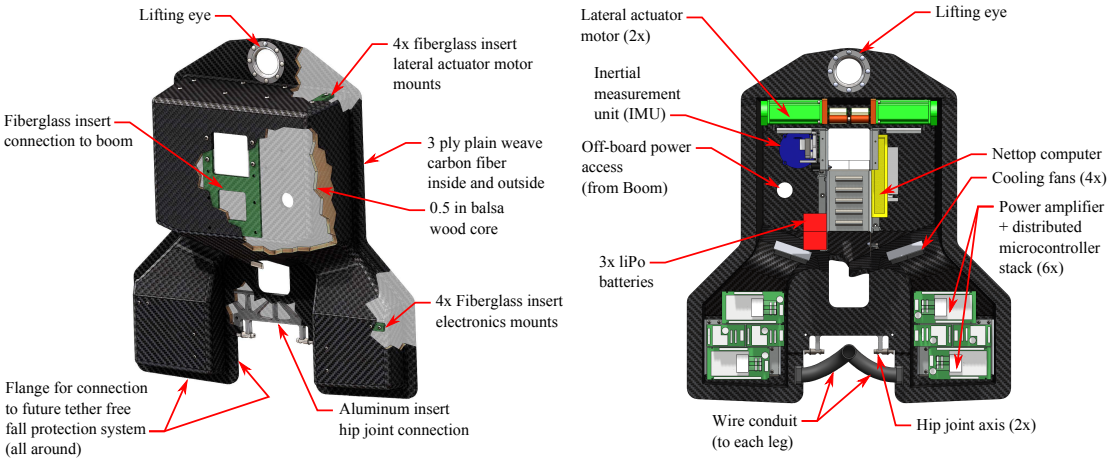

Figure 3.4: (a) Construction details of the body to make it a strong protective shell to house the various components of the robot (cover half not shown for clarity). (b) Layout of components secured to the structure half of the protective body shell.

cleanly to the left or right. These pins and screws are easily and quickly replaced. Designed into the knee but as yet untested are strain gauges that measure this lateral forces on the leg. By measuring this lateral force the lateral actuator could be used to actively reduce this force, keeping the toe forces in plane with the leg where it is strong.

3.3.3 Design Discussion

With both the template features and robot realities satisfied and a working, real world robot is built and tested in later sections, there is a set of 'cons' to contrast against the 'pros' of the ATRIAS design stated in the section thus far.

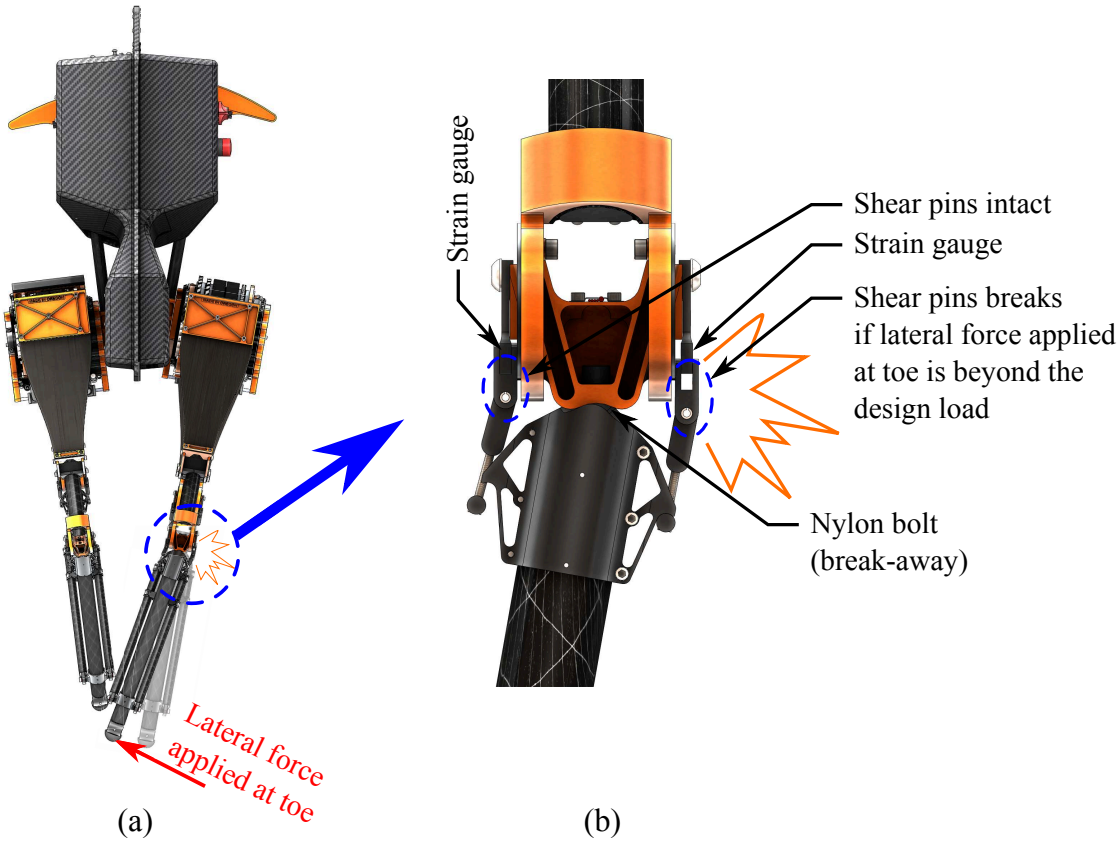

Figure 3.5: When a lateral load, F, is applied at the toe that exceeds the designed failure point a set of plastic shear pins break allowing the leg fall away and prevent higher loads from damaging other, more expensive components. This design is based around the inclusion of a set of strain gauges to measure the magnitude of these lateral forces.

3.3.3.1 Geometric Power

The leg configuration of ATRIAS with two motors driving the four-bar linkage leg has a fundamental internal power expense (geometric power, [?]) associated with swinging the leg while maintaining a force along the virtual leg length direction. During loaded leg rotation (stance phase while running or walking, Figure 3.6) both motors exert power to support the weight of the robot while the springs store and release the kinetic energy from the gait. In addition, the motors must rotate to swing the leg to allow the body to move forward. While swinging, one rotates forward, in the direction of it's applied torque, while the other rotates backwards, against it's applied torque. The sum of this (absolute) work is the geometric power required by the leg to bear the weight while swinging. This power is completely internal to the leg and does not contribute to the energy in the gait. The first motor must apply additional torque (power) to back drive the second motor to swing the leg. Thus, the ATRIAS leg design has a power overhead greater than one would expect while observing the system as a black box and calculating the power exerted by the leg by how much work it does on the world. This additional power overhead must be considered during the selection of motors and power electronics for the robot.

3.3.3.2 Mechanical efficiency

While the choice of harmonic drive transmission instead of the compound epicyclic cable drive featured on the prototype ATRIAS 1.0 was to reduce transmission

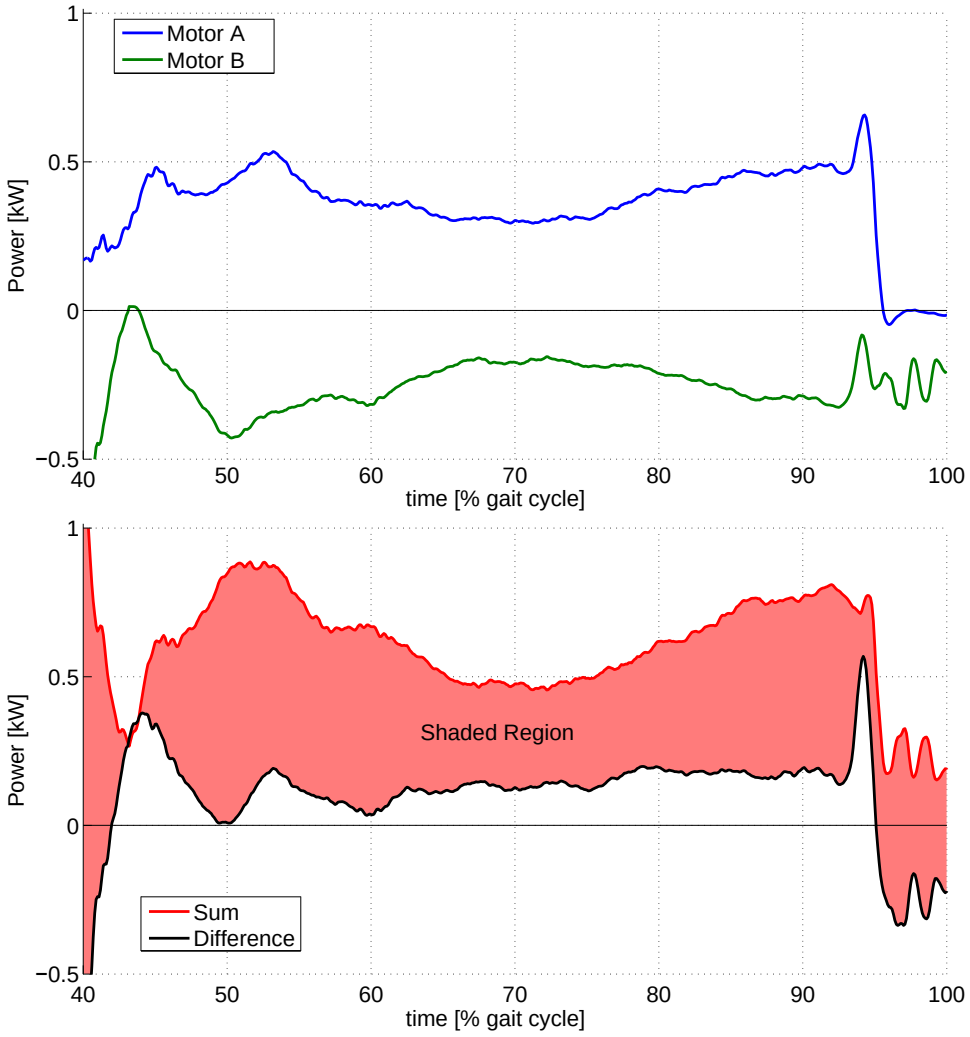

Figure 3.6: (a) Power generated by motors A and B during stance phase of a walking gait. Motor B is producing negative power for the duration. (b) The sum and difference of the absolute power produced by motor A and B. The shaded region is the Geometric power, a byproduct of the four-bar leg and motor configuration, and is an overhead power requirement necessary for the leg to maintain a holding torque while swinging the leg as is typical during stance phase during a walking or running gait.

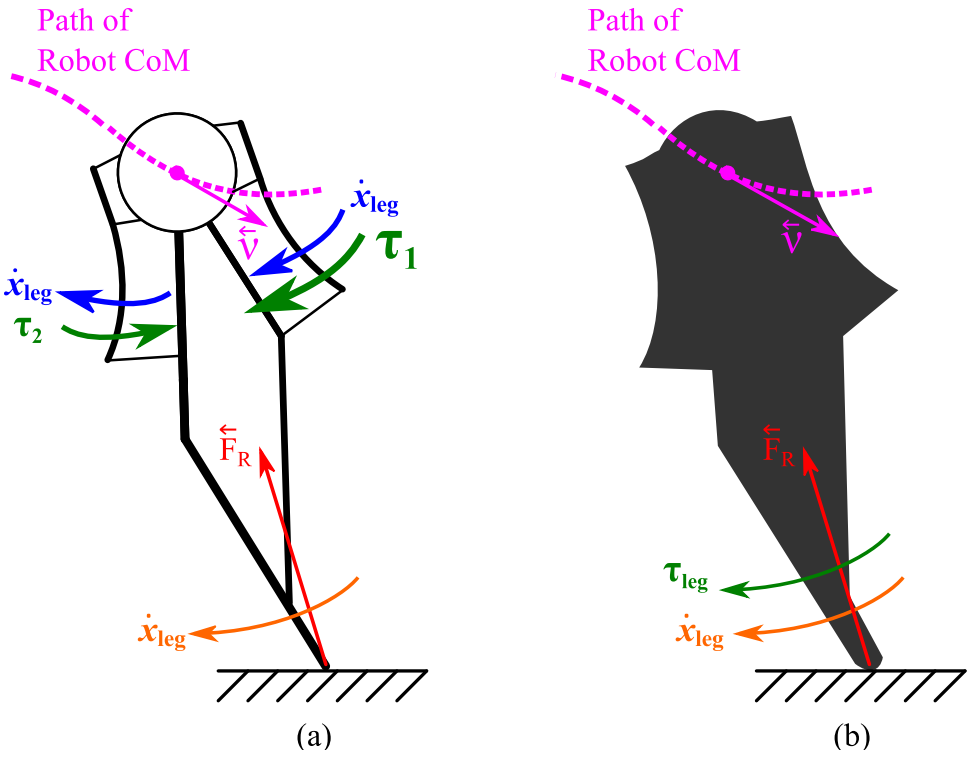

Figure 3.7: During loaded leg swing, typically stance phase, power produced by the robot (a) is greater than the power measured by an external observer (b). This is due toe the geometric work, internal to the four-bar leg and motor configuration. This impacts the design by requiring motors of greater power capacity to swing the leg through stance than if one were to not consider the geometric power.

workspace, one trade off was a reduction in mechanical efficiency. Because ATRIAS is a physical system it will have mechanical and electrical sources of energy losses and is an obligatory divergence from the spring-mass model which theoretically has no losses. One of the reasons for using the spring-mass model as the template is to take advantage of the inherent energy economy of this model to allow for locomotion with high energy economy. Thus, reducing the magnitude of losses will directly contribute to the robots energy economy.

Other sources of significant energy losses include the power electronics and motors converting stored energy in the batteries into motor torques. Wasted energy is dissipated in the form of heat.

3.3.3.3 Motor Reaction Torques

When the motors work together to swing the leg the reaction torques add causing pitching of the robot body, these torques cancel when the leg extends or retracts. This effect can be reduced with a robot configuration with an even number of legs, thus most of the time this will cancel (for symmetric gaits) but in other times will not cancel and must be accounted for in the system dynamics.

3.4 Experiments

Design constraints and real-world limitations described in Section 3.3 alter the robot's passive dynamics and necessitate active control. It is important that these

deviations are quantitatively evaluated to verify the robot will behave as intended. In order to accomplish this, we have rigorously benchmarked and validated the performance capabilities of ATRIAS. First, we describe the experimental setup used for all tests. Second, we verify that the dynamics of ATRIAS encapsulate the dynamics of our target template, the spring-mass model. Lastly, we more broadly demonstrate the performance capabilities of ATRIAS in terms of strength, versatility, robustness, and speed. Video for all experiments in this section can be found HERE.

3.4.1 Experimental Setup

The robot is supported during each experiment by a boom that restricts the robot to a circular path, measures it's position and catches it when it falls. Each axis of the boom features an encoder to measure the unrestricted motion of the robot with respect to world coordinates: the robots position and angle on the sagittal plane. These sensors play the role of an inertial measurement unit that would be installed on the robot if it were performing a 3D experiment. It should be noted that the planarization provided by the boom is in fact restricting the robots sagittal plane to be tangent to the surface of a sphere [**?**]. Additionally, the boom can be set to restrict the pitch of the robot body as well as the horizontal position of the robot.

Ground reaction forces presented in this paper are measured with a forceplate that is mounted flush with the laboratory floor. Typically used in biomechanics labs for gait analysis, this forceplate (OR6-7-4000, AMTI, Watertown, MA, USA)

measures forces (x, y and z) and moments (M_x, M_y and M_z) applied to its surface.

3.4.2 Template Validation

3.4.2.1 Passive Drop

The ideal SLIP model has zero losses and has the potential to bounce indefinitely when dropped. We know this is not the case for ATRIAS as there are impact, friction and damping losses. In this test scenario, we evaluate the magnitude of these losses through passive bouncing. We constrain movement to the vertical direction and drop ATRIAS from a fixed height ($5cm$) with a mechanically fixed leg length ($84cm$) allowing the springs to absorb the impact.

The center of mass trajectory shows a clear deviation from the SLIP model as depicted in Figure 3.8. When dropped from $5cm$, the robot returns to a height of $2.4cm$ on the next apex. Looking at the potential energy lost between these subsequent apexes, we determine a coefficient of restitution of 69.0 percent.

A key feature of the ATRIAS configuration is the apparent falling-rate leg length stiffness resulting from the non-linear geometric relations. Even with linear rotational leaf springs this non-linearity is quite pronounced as depicted in the force-length curve in Figure 3.9. We can see the previously derived (ATRIAS 1.0 paper ref?) theoretical force-length relation matches very closely to the experimental measurements with one difference. In the experimental data we see hysteresis associated with dissipative leg losses. This is expected and slowly removes energy

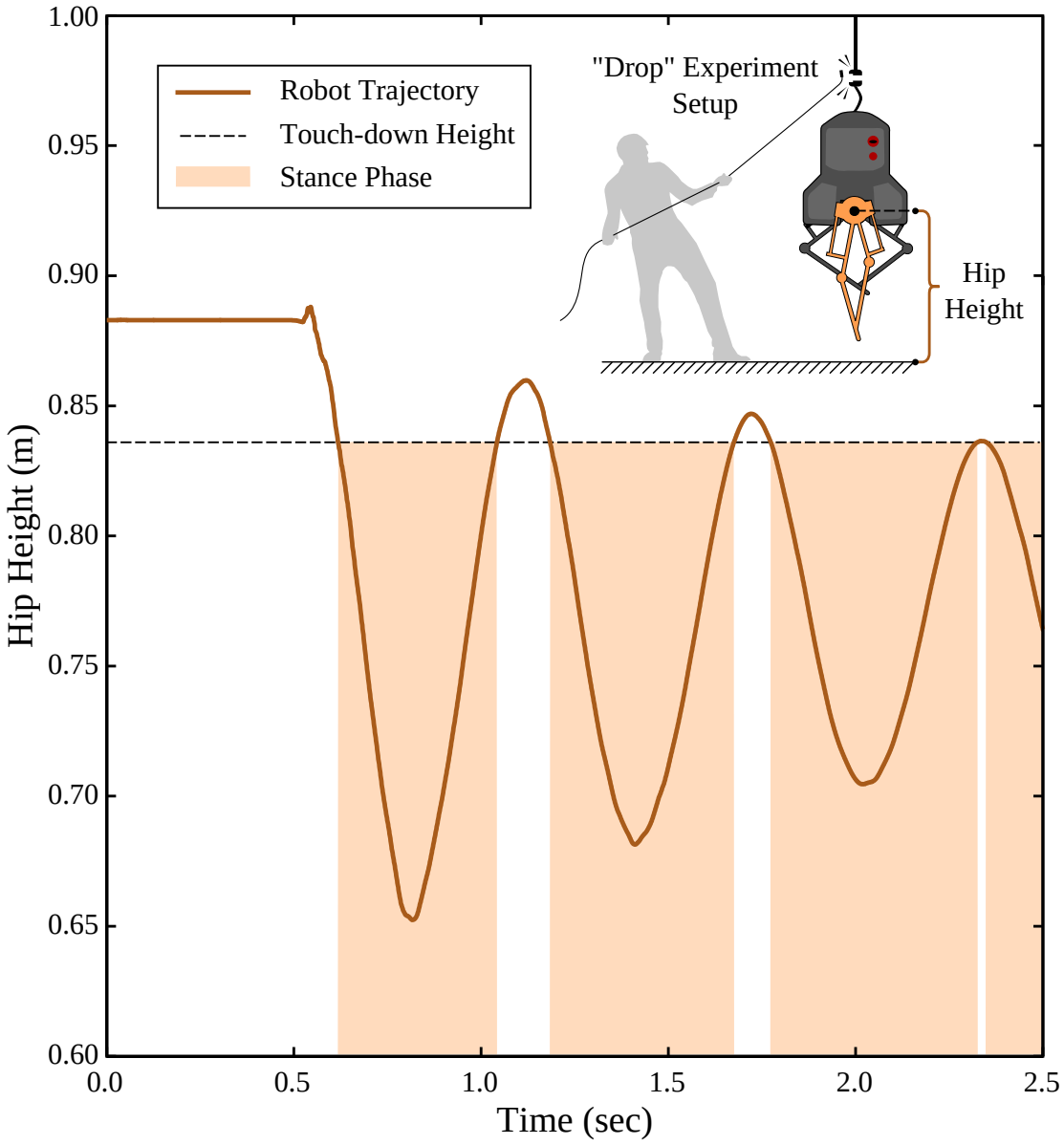

Figure 3.8: The center of mass position (red line) during the passive drop test is shown with the stance phases highlighted (gray shaded regions).

from the system that must be added back through active control later.

We can determine the magnitude of dissipation by fitting the experimental data to a modified version of our template model that includes damper in parallel to the spring. Figure 3.10 illustrates a comparison to the fit model parameters, $m = 59.9[kg], k = 6,543[N/m], c = 38.0[N/m^2], and\ \zeta = 0.0607$.

3.4.2.2 Passive Walking

An objective of ATRIAS is to implement, and test in the real world, controllers developed for the spring-mass model for walking and running. This bridges the gap between simulation work done on the SLIP model and testing these controllers in the real world. The experiment at hand aims to place one of these controllers on the robot and determine if it behaves as expected, producing similar ground reaction forces and center of mass trajectory to the SLIP model.

The controller simply controls the swing leg trajectory such that it impacts the ground at a leg length and angle that, in simulation, leads to a periodic gait. During stance, we control the legs to behave passively and apply only axial forces. Because no energy is purposefully being injected through control, a walk must be initiated by pushing the robot. Once at the target speed (1 m/s), pushing can be stopped and the robot will continue to take several steps (in this case 13 steps) before slowing to a stop. This not only shows how a simple SLIP model controller can be applied to ATRIAS, but also demonstrates it's passively efficient dynamics. We can see in Figure 3.11 the double hump vertical force profile commonly associated

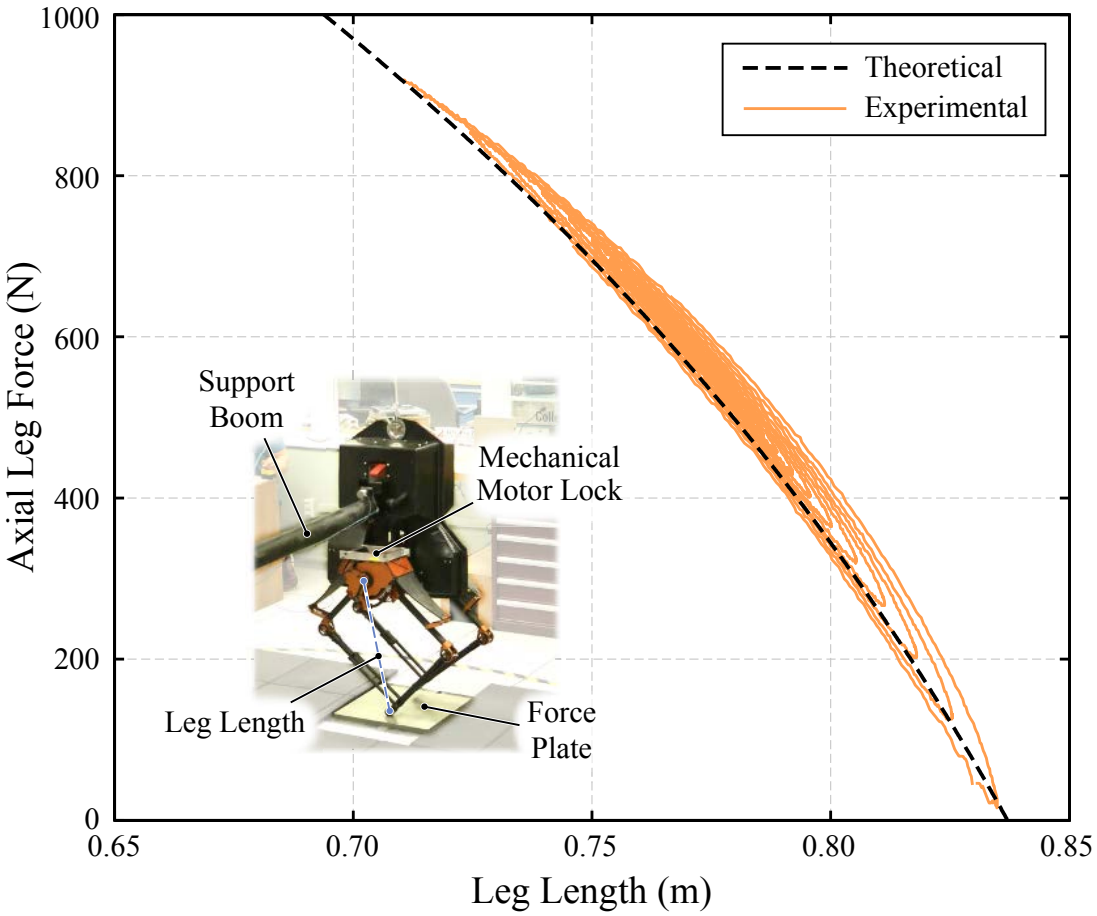

Figure 3.9: Axial leg force versus leg length measurements (red line) and the approximated non-linear function (black line) are depicted.

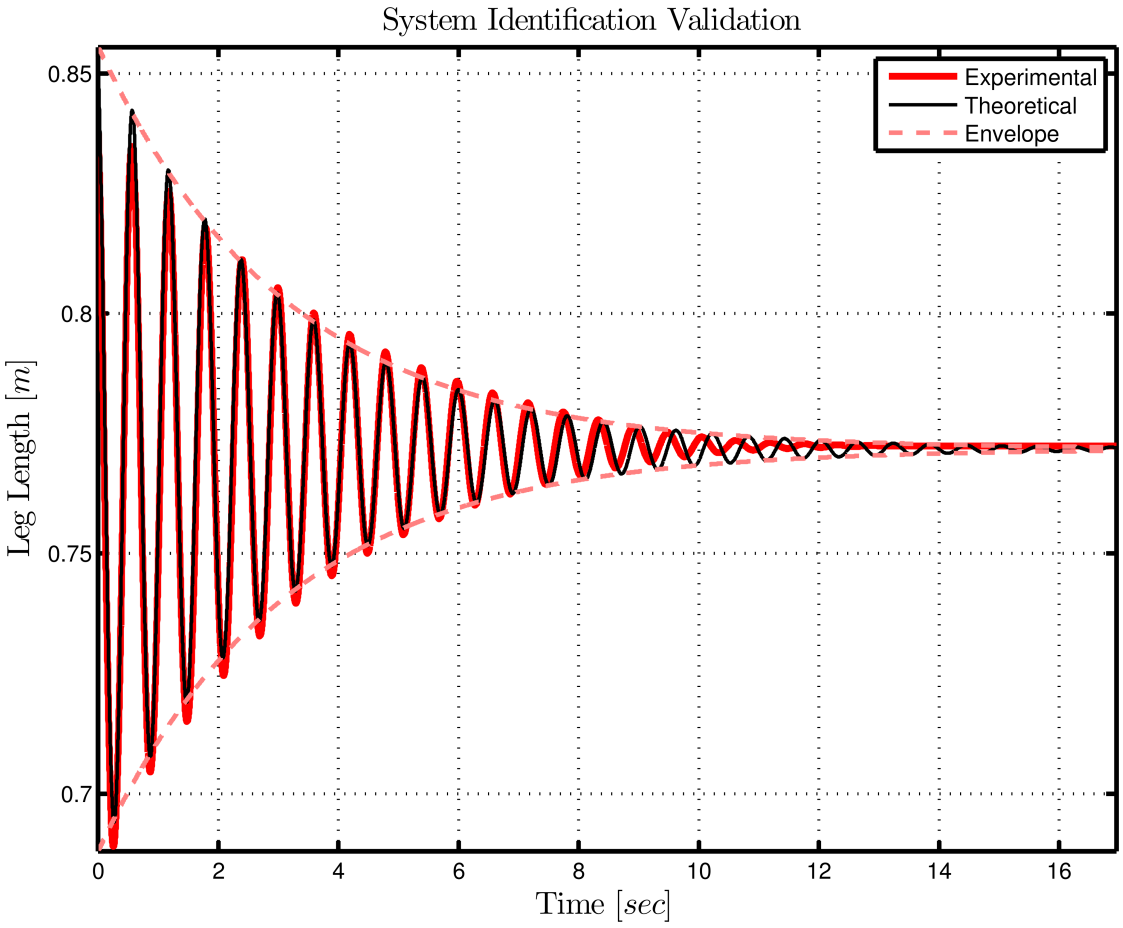

Figure 3.10: Measured versus simulated response to the system identification test. The underlining red line shows the measured response, the overlaying shaded black line shows the simulated response using best fit dynamic properties, and the dashed pink line depicts the simulated response envelope.

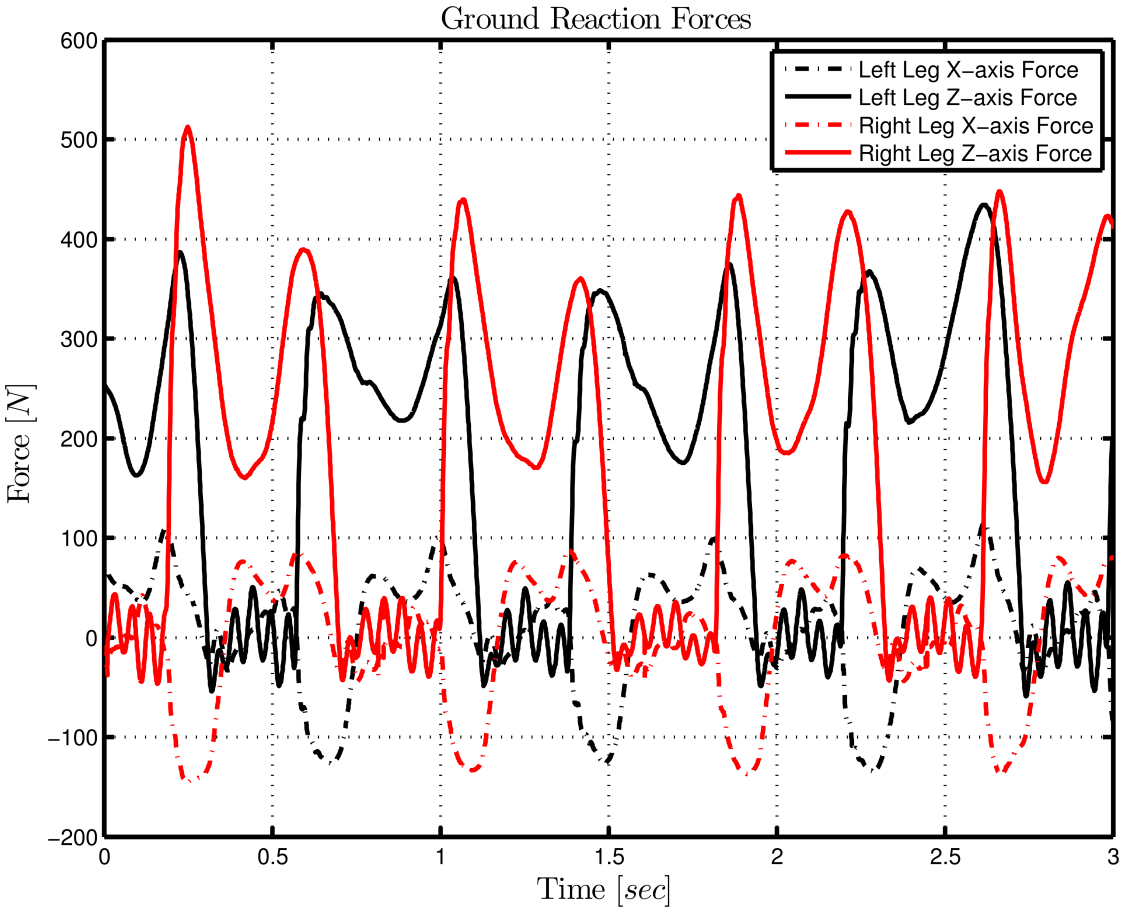

Figure 3.11: Sample of the ground reaction forces from the walking experiments. Notice the double hump....

with SLIP walking gaits.

3.4.3 Performance Demonstration

3.4.3.1 Robot Throw

In order to demonstrate compliant running on a single leg, the motors are controlled to keep the deflection of both springs symmetric during stance, thus only generating forces in leg direction by coordinating the two series elastic actuators to have equal and opposite torques on the leg. Initially and during each flight phase the leg is reset to a constant touch-down angle.

The experiment is initiated by throwing the robot thus providing its initial momentum, allowing the robot to bounce several times. The horizontal momentum rotates the leg as a result of the controllers effort to keep the spring deflection symmetric.

The robot performed several hops and covered a distance of about 6m. No energy is intentionally replenished and therefore the hopping height and forward speed decay over time (fig). As intended the force points in the direction of the leg axis at all times (fig).

3.4.3.2 Hop in Rocks

ïż£

This experiment was designed to validate the mechanical robustness, agility, and force tracking capability in a real world scenario. Using a simple PD feed-forward force controller during stance phase, the hopping height is regulated by

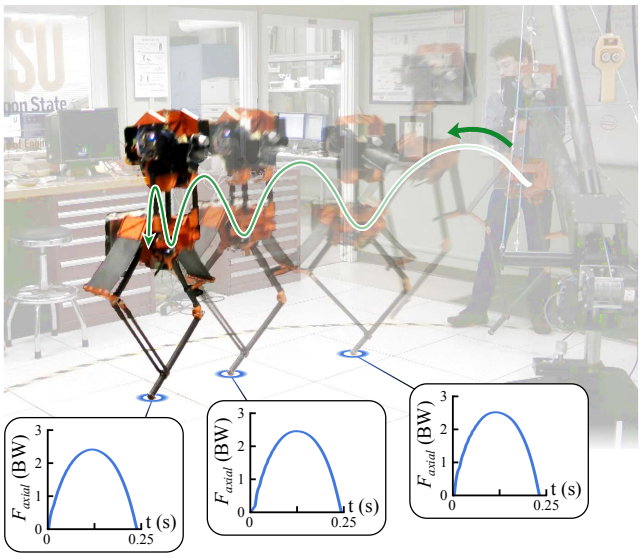

Figure 3.12: Demonstrating spring-mass hopping dynamics of the monopod, ATRIAS 2.0, exploiting the spring-mass dynamics.

tracking pre-computed ideal spring-mass force profiles. During flight, a PD position controller returns the leg to a pre-determined constant leg length and angle. After achieving a steady-state hop on flat-rigid ground, the robot is pushed into hole a filled with rocks. Despite a change in ground stiffness, damping, and height, ATRIAS was able to reject the disturbance and maintain a reasonably constant hopping height.

3.4.3.3 Sustained Walking

Walking is a sequence of alternating stance and flight phases oscillating each leg back and forth and the opposite leg essentially mirroring this motion. The con-

troller is based on a state machine, triggered by the leg currently in stance reaching a predefined extreme angle. This initiated the phase transition for both legs.

During stance the leg has to support and propel the body. The motors generate holding torques allowing the springs to be loaded and to redirect the trunk's vertical motion thus supporting the robot's weight during the stride. A hip torque is generating by distributing the holding torque unevenly between the motors rotating the leg and propelling the robot forward.

Once the stance leg reaches the predefined extreme angle the leg transistions into flight. In a first phase the parallel chain of both legs on the ground is dissolved minimising constraining forces. During the second phase the leg swings forward while getting shorter to ensure sufficient ground clearance and extending again towards the end of swing. In the last phase the swing is retracted towards the next touch-down. Timing of motion and phasing is based on the stance leg motion introducing a virtual constraint.

Each experiment started from a standing position with both legs at their extreme hip angles. A phase shift has been manually initiating causing the leading leg to go through stance phase and the trailing leg to be swung forward. Subsequently, phases shifted automatically bringing the robot into a steady motion.

The robot exhibited compliant walking generating ground reaction force profile similar to those observed in human walking. To our knowledge these characteristic double-humped force pattern have not been reported for robots.

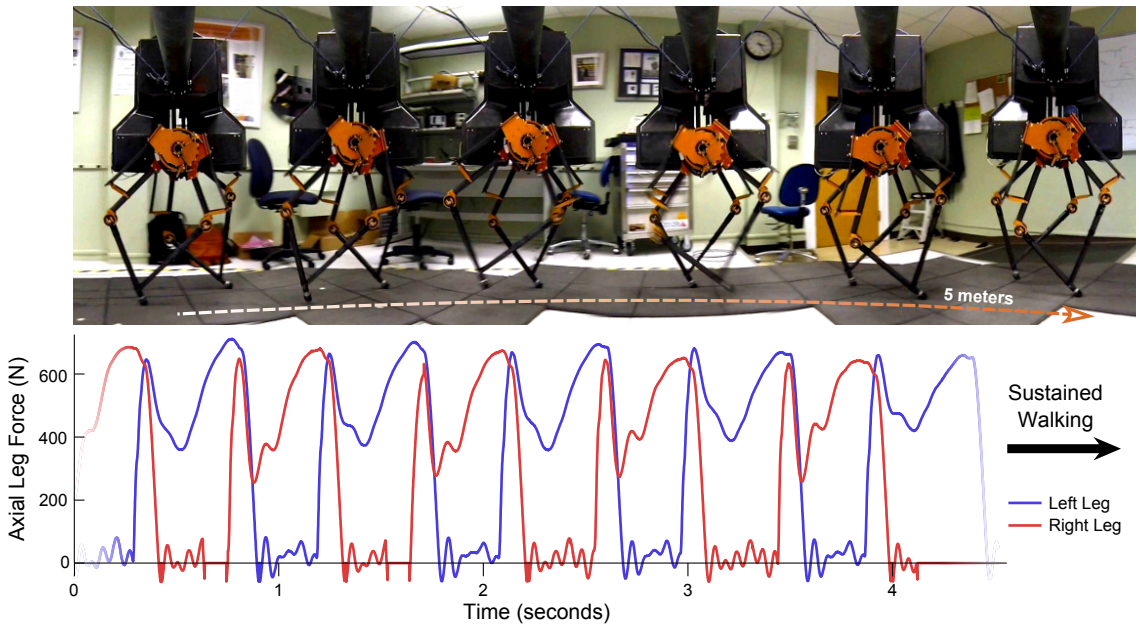

Figure 3.13: An ATRIAS walking gait and associated axial leg forces, demonstrating that sustained walking is viable for ATRIAS while sporting the characteristic "double-humped" force profile of spring-mass walking.

3.4.3.4 Single Leg Hop

Robots operating in the real world will often encounter rough environments and unseen objects while locomotion. In these cases the robot may be required energetically hop over an obstacle or absorb an impact without causing damaging itself. These requires strong actuation capabilities while preserving a soft interface with the ground. To validate ATRIAS can handle such situations, we created a single leg hopping test. In this test ATRIAS starts from standing position and begins energetically hopping on one leg using a SLIP based force controller. Within one hop ATRIAS reached a height of over $9cm$, and can continue hopping at this height without issue for several minutes. This is a monumentally success, and demonstrates the energetic capabilitie4s of ATRIAS.

3.5 Conclusion

We present ATRIAS as an example of applying template-driven design to a versatile, human-scale bipedal robot. By leveraging a low-mass fourbar leg mechanism and series-elastic plate springs, ATRIAS exhibits spring-mass locomotion when pushed or thrown. Applying limited-work control to ATRIAS allows for both sustained walking and hopping, demonstrating a capability for executing a variety of gaits (a limitation of prior template driven robots). This versatility included hopping into, and out of, an unseen 6.5-inch-deep gravel pit, demonstrating notable control authority.

ATRIAS is the first documented bipedal machine to replicate the human-

like ground reaction forces of spring-mass walking. This characteristic "double-humped" force profile was measured both during a 14-step "passive" walk (using a near-zero-work leg controller) and a sustained steady walking (using a simple proof-of-concept walking controller). This result advances a broader point regarding bioinspired robot design. Robot mechanisms need not be morphologically biomimetic (e.g. ATRIAS' spring-loaded fourbar leg mechanism) in order to produce biologically relevant dynamics (human ground-reaction forces). Further, these human-like dynamics emerge from efficient control of appropriately designed passive dynamics, and do not necessarily need to be the explicit target of a feedback control loop.

The template-driven design approach is paramount to ATRIAS' dynamical capabilities. The extent to which it performs varied motions are predicted by the spring-mass model. ATRIAS also embodies an extension of template dynamics to more practical machines, avoiding the limitations of rigidity and actuation typical to humanoid robots. It demonstrates that template-driven robots are not limited to laboratory platforms. On the contrary, at a time when humanoid robots are too inefficient and dynamically encumbered to be practical, the additional design challenges of the template-driven approach may prove necessary for legged robots to achieve the agility and economy of animals.

3.6 Future Work

ïż£

The template driven approach to robot design presented in this paper has yielded a robot that is unique and very well suited for its intended task of being a platform for legged locomotion research centered around the spring-mass model. Performance of ATRIAS exceeds that of legged robots designed around a more traditional approach yet still has issues that the authors believe can be rectified. Powerlooping, for example, is a byproduct of ATRIAS's arrangement of motors with the four-bar linkage leg. Working through the template driven approach to robot design a different leg configuration can be explored that could also dynamically match the spring-mass model while avoiding powerlooping.

Future work with ATRIAS will involve the further research and development of controllers to test existing theory simulated on the spring-mass model. The hope is to prove that we have a fundamental insight into the solution for legged locomotion. Results of this future work will allow ATRIAS to locomote with high energy efficiency with very robust controllers over a variety of obstacles. <3D... untethered... unsupported... etc>

Acknowledgment

The authors would like to thank Kit Morton, Ryan Van-Why, Soo-Hyun, Ethan Shepard for their dedicated work in building ATRIAS, it's electronics and software systems as well as the upgrading the support boom. Thanks to Oregon State University. And thanks to the machine shops and composites shops for fabricating the components of ATRIAS.

The Authors would also like to thank their collaborators at the University of Michigan, Jessy Grizzle, as well as their collaborators at Carnegie Mellon Universities Robotics Institute, Hartmut Geyer.

Special thanks is given to DARPA project director Gill Pratt and DARPA grant #W91CRB-11-1-0002.

Appendix

The appendix of this paper is moved to the appendix of the Thesis in order to follow formatting guidelines of the University. Please see Appendix B

Chapter 4 – Conclusion

In the work for this thesis three identical human scale biped robots were developed, constructed and deployed to three different research labs across the United States: Oregon State University, University of Michigan, and the Robotics Institute at Carnegie Mellon University. ATRIAS will serve as a research platform for the exploration and realization of the spring-mass model for legged locomotion's potential for that role. The passive dynamics of this robot are designed specifically to match that of the spring-mass model so that controller ideas and methods vetted in simulation in the literature can be validated in the real world. Further ideas and methods can be implemented on ATRIAS in the hopes of creating an energetically efficient and robust walking and running robot.

4.1 Towards the Goal of Selecting Motors for a Robot

Motor inertia is as important, or more than, peak torque or speed when choosing a motor. The inertia of the motor has a strong effect on the motor and system bandwidth. For higher bandwidth one should seek to decrease motor inertia, J. Thinking of J as the simple equation $\frac{b \cdot h^2}{12}$ the most influential term on the inertia is h, or the radius of the motor rotor. To minimize motor inertia J, one must minimize h. Inertia of the motor is important due to the amplification of the loads's inertia

reflected to, or as observed by, the motor through the gear reduction. Total inertia at the motor that will be accelerated by the motors torque is $J_{total} = \frac{J_{load}}{N^2} + J_{motor}$ where N is the gear ratio. If N is large then the motor inertia, J_{motor}, will dominate J_{total}. For servo drive applications it is recommended that J_{load} and J_{motor} be sized such that they have a 1:1 ratio for maximized controllability. With the decision to use harmonic drive's as the transmission in ATRIAS the design was limited to a minimum of 50:1 gear ratio. This skewed the J_{load} and J_{motor} radio and results in a motor inertia that dominates while in flight phase (just the inertia of the lightweight four-bar leg). For stance phase the load is greater (the whole weight of the robot) and thus the load dominates. So, the 50:1 ratio is a sort of compromise for this hybrid system where a low gear ratio is desired for flight phase (low inertia load) and a high gear ratio for stance phase (high inertia load). A third consideration is the impact at the end of flight phase and beginning of stance phase. Here your are effectively catching the large load inertia. For this case a low motor inertia is good for the transient of catching the large load and entering stance phase where you'd want a high gear ratio.

4.2 Conclusion of Chapter 2

In the journal paper included in Chapter 2, we introduce the concept of and reasons for the development of the ATRIAS 1.0 prototype. We show how the features of the template model are reproduced in a physical system with actuators to allow for robust locomotion. A number of novel contributions from this work is the

use of a lightweight yet strong four-bar linkage in place of the typical two-link leg found in many other robots and is a good approximation of the massless leg from the template spring-mass model. Series compliance is achieved with plate springs arranged in with the four-bar and are placed in series between the leg and the motors. A novel transmission is developed for ATRIAS 1.0, the compound epicyclic cable drive, providing high force transmission with zero-backlash for a low weight. Through several engineering tests to validate the system design, the machine demonstrated spring-mass behavior, successfully achieving the goal of generating passive dynamics that match a simple, controllable reduced-order model.

4.3 Conclusion of Chapter 3

In the second journal paper included in this thesis, Chapter 3, we in present the completed biped version of ATRIAS, version 2.1. In this paper we show the biped configuration for this tether free, 3D capable robot. Early experimentation results are included with the paper that seek to validate the robots intended passive dynamics: to match the spring-mass model. These tests include a vertical hopping test that is exactly the situation that is proven as an analytical match in the first paper, Appendix A. A passive walk experiment is performed with the robot and seeks to bridge the gap between simulation work done with the spring-mass model and testing controllers for that system in the real world. The paper also includes a set of demonstrations that give light to the robots ability to do tasks, such as

running, leaping and disturbance rejection. While not thorough experiments with properly developed controllers and strategies, these give an indication as to the robots ability to do these tasks, with little effort. In time these goals will be fully tested and proper controllers will be developed to seek the limits of the potential of the ATRIAS concept for robotic legged locomotion

Bibliography

[1] H. Geyer, A. Seyfarth, and R. Blickhan, "Positive force feedback in bouncing gaits?" in *Proceedings of Biological Sciences*, vol. 270, no. 1529, October 2003, pp. 2173–2183.

[2] ——, "Compliant leg behaviour explains basic dynamics of walking and running," *Proceedings of the Royal Society B-Biological Sciences*, vol. 273, no. 1603, pp. 2861–2867, 2006.

[3] H. Geyer, R. Blickhan, and A. Seyfarth, "Natural dynamics of spring-like running – emergence of selfstability," in *Proceedings of the 5th international conference on climbing and walking robots*. Professional Engineering Publishing Limited, 2002, pp. 87–92.

[4] R. Blickhan, "The spring-mass model for running and hopping," *J. of Biomech.*, vol. 22, no. 11/12, pp. 1217–1227, 1989.

[5] M. Ahmadi and M. Buehler, "Controlled passive dynamic running experiments with the ARL Monopod II," *IEEE Trans. on Robotics*, vol. 22, no. 5, pp. 974–86, Oct. 2006.

[6] B. Brown and G. Zeglin, "The bow leg hopping robot," in *Robotics and Automation, 1998. Proceedings. 1998 IEEE International Conference on*, vol. 1, May 1998, pp. 781 –786 vol.1.

[7] M. H. Raibert, *Legged Robots That Balance*. Cambridge: MIT Press, 1986.

[8] M. Vucobratovič and B. Borovac, "Zero-moment point–thirty five years of its life," *Intl. J. of Humanoid Robotics*, vol. 1, pp. 157–73, 2004.

[9] M. Ernst, H. Geyer, and R. Blickhan, "Spring-legged locomotion on uneven ground: a control approach to keep the running speed constant." in *Proc 12th Int Conf on Climbing and walking Robots (CLAWAR)*, 2009, pp. 639–644.

[10] R. Blickhan, "The spring mass model for running and hopping," *J. of Biomech.*, vol. 22, no. 11–12, pp. 1217–27, 1989.

[11] A. Seyfarth, H. Geyer, and H. Herr, "Swing-leg retraction: a simple control model for stable running," *The Journal of Experimental Biology*, pp. 2547–2555, 2003.

[12] A. Seyfarth, H. Geyer, M. Guenther, and R. Blickhan, "A movement criterion for running," *Journal of Biomechanics*, vol. 35, pp. 649–655, 2002.

[13] R. M. Ghigliazza, R. Altendorfer, P. Holmes, and D. Koditschek, "A simply stabilized running model," *SIAM Journal on Applied Dynamical Systems*, vol. 2, pp. 187–218, 2003.

[14] H. Geyer, A. Seyfarth, and R. Blickhan, "Spring-mass running: Simple approximate solution and application to gait stability," *Journal of Theoretical Biology*, vol. 232, pp. 315–328, 2005.

[15] M. Ernst, H. Geyer, and R. Blickhan, "Extension and customization of self-stability control in compliant legged systems," *Bioinspiration & Biomimetics*, vol. 7, no. 4, p. 046002, 2012.

[16] J. Schmitt, M. Garcia, R. C. Razo, P. Holmes, and R. J. Full, "Dynamics and stability of legged locomotion in the horizontal plane: A test case using insects," *Biological Cybernetics*, vol. 86, pp. 343–353, 2002.

[17] J. Rummel, Y. Blum, and A. Seyfarth, "Robust and efficient walking with spring-like legs," *Bioinspiration & Biomimetics*, vol. 5, no. 4, p. 046004, 2010.

[18] B. Miller, J. Schmitt, and J. E. Clark, "Quantifying disturbance rejection of slip-like running systems," *The International Journal of Robotics Research*, vol. 31, no. 5, pp. 573–587, 2012.

[19] R. Blickhan and R. J. Full, "Similarity in multilegged locomotion: Bouncing like a monopode," *J. of Comparative Physiology*, pp. 509–17, 1993.

[20] C. T. Farley, J. Glasheen, and T. A. McMahon, "Running springs: Speed and animal size," *J. of Experimental Biology*, pp. 71–86, 1993.

[21] R. J. Full and C. T. Farley, "Musculoskeletal dynamics in rhythmic systems - a comparative approach to legged locomotion," in *Biomechanics and Neural Control of Posture and Movement*, J. M. Winters and P. E. Crago, Eds. New York: Springer-Verlag, 2000.

[22] J. R. Hutchinson, D. Famini, R. Lair, and R. Kram, "Are fast-moving elephants really running?" *Nature*, vol. 422, pp. 493–4, 2003.

[23] T. A. McMahon and G. C. Cheng, "The mechanics of running: How does stiffness couple with speed?" *J. of Biomech.*, vol. 23, pp. 65–78, 1990.

[24] A. Seyfarth, H. Geyer, M. Gunther, and R. Blickhan, "A movement criterion for running," *J. of Biomech.*, vol. 35, pp. 649–55, Nov. 2001.

[25] A. Goswami, B. Thuilot, and B. Espiau, "Compass-like biped robot part I : Stability and bifurcation of passive gaits," 1996, rapport de recherche de l'INRIA.

[26] B. Espiau and A. Goswami, "Compass gait revisited," in *Proc. of the IFAC Symposium on Robot Control*, Capri, Sep. 1994, pp. 839–46.

[27] I. A. Hiskens, "Stability of hybrid limit cycles: application to the compass gait biped robot," in *40th IEEE Conf. on Decision and Control*, Orlando, Dec. 2001, pp. 774–9.

[28] K. Byl and R. Tedrake, "Approximate optimal control of the compass gait on rough terrain," in *IEEE Intl. Conf. on Robotics and Automation*, Pasadena, May 2008.

[29] M. Garcia, A. Chatterjee, A. Ruina, and M. Coleman, "The simplest walking model: stability, complexity and scaling," *ASME J. of Biomech. Eng.*, vol. 120, no. 2, pp. 281–8, Apr. 1998.

[30] A. D. Kuo, "Energetics of actively powered locomotion using the simplest walking model," *J. of Biomech. Eng.*, vol. 124, pp. 113–20, 2002.

[31] G. Bessonnet, S. Chessé, and P. Sardain, "Optimal gait synthesis of a seven-link planar biped," *The International Journal of Robotics Research*, vol. 23, no. 10–11, pp. 1059–73, 2004. [Online]. Available: http://ijr.sagepub.com/content/23/10-11/1059.abstract

[32] P. N. Mousavi and A. Bagheri, "Mathematical simulation of a seven link biped robot on various surfaces and ZMP considerations," *Applied Mathematical Modelling*, vol. 31, no. 1, pp. 18–37, 2007. [Online]. Available: http://www.sciencedirect.com/science/article/pii/S0307904X06001612

[33] J. Furusho and A. Sano, "Sensor-based control of a nine-link biped," *Intl. J. of Robotics Research*, vol. 9, no. 2, pp. 83–98, 1990. [Online]. Available: http://ijr.sagepub.com/content/9/2/83.abstract

[34] P. Holmes, R. J. Full, D. E. Koditschek, and J. Guckenheimer, "The dynamics of legged locomotion: Models, analyses, and challenges," *SIAM Review*, vol. 48, no. 2, pp. 207–304, May 2006.

[35] J. Schmitt and P. Holmes, "Mechanical models for insect locomotion: Stability and parameter studies," *Physica D.*, vol. 156(1-2), pp. 139–168, 2001.

[36] W. J. Schwind, "Spring loaded inverted pendulum running: A plant model," Ph.D. dissertation, University of Michigan, 1998.

[37] M. Ahmadi and M. Buehler, "A control strategy for stable passive running," in *IEEE Conf. on Intelligent Systems and Robots*, 1995, pp. 152–7.

[38] I. Poulakakis and J. W. Grizzle, "The spring loaded inverted pendulum as the hybrid zero dynamics of an asymmetric hopper," *IEEE Trans. on Automatic Control*, vol. 54, no. 8, pp. 1779–93, Aug. 2009.

[39] J. Guckenheimer and P. Holmes, *Nonlinear Oscillations, Dynamical Systems, and Bifurcations of Vector Fields*, 2nd ed., ser. Applied Mathematical Sciences. New York: Springer-Verlag, 1996, vol. 42.

[40] G. Zeglin and H. B. Brown, "Control of a bow leg hopping robot," in *IEEE Intl. Conf. on Robotics and Automation*, May 1998.

[41] H. Geyer, A. Seyfarth, and R. Blickhan, "Compliant leg behaviour explains the basic dynamics of walking and running," *Proc. R. Soc. Lond. B.*, vol. 273, pp. 2861–7, 2006.

[42] R. M. Alexander, "Tendon elasticity and muscle function," *Comparative Biochemistry and Physiology a-Molecular and Integrative Physiology*, vol. 133, no. 4, pp. 1001–1011, 2002.

[43] A. A. Biewener and M. A. Daley, "Unsteady locomotion: integrating muscle function with whole body dynamics and neuromuscular control," *J. of Experimental Biology*, vol. 210, pp. 2949–60, 2007.

[44] M. A. Daley, G. Felix, and A. A. Biewener, "Running stability is enhanced by a proximo-distal gradient in joint neuromechanical control." *J. of Experimental Biology*, vol. 210, pp. 383–94, 2007.

[45] A. M. Wilson, M. P. McGuigan, A. Su, and A. J. van den Bogert, "Horses damp the spring in their step," *Nature*, vol. 414, no. 6866, pp. 895–9, 2001.

[46] M. W. Spong and F. Bullo, "Controlled symmetries and passive walking," *IEEE Trans. on Automatic Control*, vol. 50, no. 7, pp. 1025–31, Jul. 2005.

[47] M. Spong, "Passivity based control of the compass gait biped," in *14th IFAC World Congress*, Beijing, Jul. 1999.

[48] M. W. Spong, "Partial feedback linearization of underactuated mechanical systems," in *IEEE/RSJ Intl. Conf. on Intelligent Robots and Systems*, Munich, Sep. 1994, pp. 314–321.

[49] T. Yang, E. R. Westervelt, A. Serrani, and J. P. Schmiedeler, "A framework for the control of stable aperiodic walking in underactuated planar bipeds," vol. 27, no. 3, pp. 277–290, 2009.

[50] J. A. Rosas-Flores, J. Alvarez-Gallegos, and R. Castro-Linares, "Stabilization of a class of underactuated systems," in *39th IEEE International Conference on Decision and Control*, Sydney, Dec. 2000, pp. 2168–73.

[51] R. Altendorfer, R. M. Ghigliazza, and P. Holmes, "Exploiting passive stability for hierarchical control," in *5th Intl. Conf. on Climbing and Walking Robots*, Paris, 2002, pp. 177–84.

[52] A. Goswami, B. Espiau, and A. Keramane, "Limit cycles in a passive compass gait biped and passivity-mimicking control laws." *J. of Autonomous Robots*, vol. 4, pp. 273–286, 1997.

[53] G. A. Pratt and M. M. Williamson, "Series elastic actuators," in *IEEE International Conference on Intelligent Robots and Systems*, vol. 1, 1995, pp. 399–406.

[54] J. Pratt and G. Pratt, "Exploiting natural dynamics in the control of a planar bipedal walking robot," in *Proceedings of the Thirty-Sixth Annual Allerton Conference on Communication, Control, and Computing*, September 1998.

[55] D. Koepl, K. Kemper, and J. Hurst, "Force control for spring-mass running and walking," in *IEEE Conference on Advanced Intelligent Mechatronics*, July 2010.

[56] K. Kemper, D. Koepl, and J. Hurst, "Optimal Passive Dynamics for Torque/Force Control," in *International Conference on Robotics and Automation*, 2010.

[57] D. Koepl, K. Kemper, and J. Hurst, "Force control for spring-mass walking and running," in *Advanced Intelligent Mechatronics (AIM), 2010 IEEE/ASME International Conference on*, Jul. 2010, pp. 639–644.

[58] D. Koepl and J. Hurst, "Force Control for Planar Spring-Mass Running," in *IEEE International Conference on Intelligent Robots and Systems*, 2011.

[59] C. Hubicki and J. W. Hurst, "Running on soft ground: simple, energy-optimal disturbance rejection," in *CLAWAR 2012*, 2012, pp. 543–547.

[60] H. R. Vejdani and J. W. Hurst, "Swing leg control for actuated spring-mass robots," in *CLAWAR 2012*, July 2012, pp. 536–542.

[61] T. McGeer, "Passive dynamic biped catalog," in *2nd Intl. Symposium of Experimental Robotics*, Toulouse, 1991, pp. 465–90.

[62] S. H. Collins, M. Wisse, and A. Ruina, "A three-dimensional passive-dynamic walking robot with two legs and knees," *Intl. J. on Robotics Research*, vol. 20, no. 7, pp. 607–15, Jul. 2001.

[63] S. H. Collins, A. Ruina, R. Tedrake, and M. Wisse, "Efficient bipedal robots based on passive dynamic walkers," *Science Magazine*, vol. 307, no. 5712, pp. 1082–5, 2005.

[64] M. Vukobratovič, B. Borovac, and V. Potkonjak, "ZMP: A review of some basic misunderstandings," *Intl. J. of Humanoid Robotics*, vol. 3, no. 2, pp. 153–175, June 2006.

[65] S. Kajita, M. Morisawa, K. Harada, K. Kaneko, F. Kanehiro, K. Fujiwara, and H. Hirukawa, "Biped walking pattern generation by using preview control of zero-moment point," vol. 2, Taipei, Taiwan, 2003, pp. 1620–1626.

[66] T. McGeer, "Passive dynamic walking," *Intl. J. Robotics Research*, vol. 9, no. 2, pp. 62–82, 1990.

[67] M. J. Coleman and A. Ruina, "An uncontrolled walking toy that cannot stand still," *Phys. Rev. Let.*, vol. 80, pp. 3658–61, 1998.

[68] E. Westervelt, J. Grizzle, C. Chevallereau, J. Choi, and B. Morris, *Feedback Control of Dynamic Bipedal Robot Locomotion*, ser. Control and Automation. Boca Raton: CRC Press, June 2007.

[69] J. Pratt, C.-M. Chew, A. Torres, P. Dilworth, and G. Pratt, "Virtual model control: An intuitive approach for bipedal locomotion," *The International Journal of Robotics Research*, 2001.

[70] M. Ahmadi and M. Buehler, "The ARL Monopod II running robot: Control and energetics," in *IEEE Intl. Conf. on Robotics and Automation*, Detroit, May 1999, pp. 1689–94.

[71] U. Saranli, M. Buehler, and D. E. Koditschek, "RHex: A simple and highly mobile hexapod robot," *Intl. J. Robotics Research*, vol. 20, no. 7, pp. 616–31, 2001.

[72] S. Kim, J. E. Clark, and M. R. Cutkosky, "iSprawl: Autonomy, and the effects of power transmission," in *7th Intl. Conf. on Climbing and Walking Robots (CLAWAR)*, Madrid, Sep. 2004.

[73] J. W. Hurst, J. E. Chestnutt, and A. A. Rizzi, "An actuator with physically adjustable compliance for highly dynamic legged locomotion," in *IEEE Intl. Conf. on Robotics and Automation*, New Orleans, Apr. 2004.

[74] ——, "Series compliance for an efficient running gait: Lessons learned from the ecd leg," *IEEE Robotics and Automation Magazine*, vol. Sep., pp. 42–51, 2008.

[75] K. Sreenath, H.-W. Park, I. Poulakakis, and J. W. Grizzle, "A Compliant Hybrid Zero Dynamics Controller for Stable, Efficient and Fast Bipedal Walking on MABEL," *Int. J. Rob. Res.*, vol. 30, no. 9, pp. 1170–1193, Aug. 2011. [Online]. Available: http://dx.doi.org/10.1177/0278364910379882

[76] D. W. Robinson, J. E. Pratt, D. J. Paluska, and G. A. Pratt, "Series elastic actuator development for a biomimetic walking robot," in *IEEE/ASME international conference on advanced intelligent mechatronics*, September 1999.

[77] The ABB Group, "IRB 360 FlexPicker robot," Packaging Magazine, Jul. 2008.

[78] S.-M. Song and J.-K. Lee, "The mechanical efficiency and kinematics of pantograph-type manipulators," *KSME Journal*, vol. 2, no. 1, pp. 69–78, 1988.

[79] S. I. INC., *Cable Design Info*, Sava Industries, INC. Std. [Online]. Available: www.savacable.compages/applic.html

[80] W. T. Townsend, "The effect of transmission design on force-controlled manipulator performance," Ph.D. dissertation, Massachusetts Institute of Technology, 1988.

[81] W. T. Townsend and J. K. Salisbury, "The efficiency limit of belt and cable drives," in *ASME Journal of Mechanisms, Transmissions, and Automation in Design*, vol. 110, September 1988, pp. 303–307.

[82] J. W. Hurst, "The Role and Implementation of Compliance in Legged Locomotion," PhD, Carnegie Mellon University, 2008. [Online]. Available: http://proquest.umi.com/pqdlink?Ver=1&Exp=01-26-2016&FMT=7&DID=1674914821&RQT=309&attempt=1&cfc=1

[83] M. P. Summers, *Rope Selection for Rope Drive Transmissions Used in Robotic Manipulation*, Oregon State University - University Honors College Std., August 2010. [Online]. Available: http://hdl.handle.net/1957/18379

[84] *Marlow RRope Technical Information*, Std. [Online]. Available: http://www.marlowropes.com/technical/physical-properties.html

[85] J. S. Collett and J. W. Hurst, "Artificial restraint systems for walking and running robots: An overview," *International Journal of Humanoid Robotics*, vol. 09, no. 01, p. 1250001, 2012. [Online]. Available: http://www.worldscientific.com/doi/abs/10.1142/S0219843612500016

[86] J. W. H. Andrew Peekema, Daniel Renjewski, "Open-source real-time robot operation and control system for highly dynamic, modular machines," in *ASME 2013, International Design Engineering Technical Conferences & International Conference on Multibody Systems, Nonlinear Dynamics, and Control*, 2013.

[87] R. Blickhan, "The Spring Mass Model for Running and Hopping," *Journal of Biomechanics*, vol. 22, no. 11-12, pp. 1217–1227, 1989.

[88] H. Geyer, A. Seyfarth, and R. Blickhan, "Compliant leg behaviour explains the basic dynamics of walking and running," *Proc. R. Soc. Lond. B.*, vol. 273, pp. 2861–7, 2006.

[89] J. Schmitt and P. Holmes, "Mechanical models for insect locomotion: dynamics and stability in the horizontal plane i. theory," *Biological Cybernetics*, vol. 83, pp. 501–515, 2000.

[90] A. Seyfarth, H. Geyer, and H. Herr, "Swing-leg retraction: a simple control model for stable running," *Journal of Experimental Biology*, vol. 206, no. 15, pp. 2547–2555, 2003. [Online]. Available: http://jeb.biologists.org/content/206/15/2547.abstract

[91] H. Geyer, A. Seyfarth, and R. Blickhan, "Spring-mass running: simple approximate solution and application to gait stability," *J. of Theoret. Biol.*, no. 232, pp. 315–328, 2005.

[92] J. E. Seipel and P. Holmes, "Running in three dimensions: Analysis of a point-mass sprung-leg model," *International Journal of Robotics Research*, vol. 24, pp. 657–674, 2005.

[93] R. M. Ghigliazza, R. Altendorfer, P. Holmes, and D. Koditschek, "A simply stabilized running model," *Siam Review*, vol. 47, no. 3, p. 519Ũ549, 2005.

[94] M. A. Daley, J. R. Usherwood, G. Felix, and A. A. Biewener, "Running over rough terrain: guinea fowl maintain dynamic stability despite a large unexpected change in substrate height," *J. of Experimental Biology*, vol. 209, pp. 171–187, 2006.

[95] Y. Blum, S. W. Lipfert, J. Rummel, and A. Seyfarth, "Swing leg control in human running," *Bioinspiration & Biomimetics*, vol. 5, no. 2, p. 026006, Jun. 2010.

[96] F. Peuker, C. Maufroy, and A. Seyfarth, "Leg-adjustment strategies for stable running in three dimensions," *Bioinspiration & Biomimetics*, vol. 7, no. 3, p. 036002, Sep. 2012. [Online]. Available: http://stacks.iop.org/1748-3190/7/i=3/a=036002?key=crossref.9eb9b428ad0880a48b8522517c9c9e09

[97] M. Hirose and K. Ogawa, "Honda humanoid robots development," *Philosophical Transactions of the Royal Society A: Mathematical, Physical and Engineering Sciences*, vol. 365, no. 1850, p. 11Ű19, 2007. [Online]. Available: http://rsta.royalsocietypublishing.org/content/365/1850/11.short

[98] K. Kaneko, F. Kanehiro, M. Morisawa, K. Akachi, G. Miyamori, A. Hayashi, and N. Kanehira, "Humanoid robot hrp-4-humanoid robotics platform with lightweight and slim body," in *Intelligent Robots and Systems (IROS), 2011 IEEE/RSJ International Conference on*, 2011, p. 4400Ű4407.

[99] I.-W. Park, J.-Y. Kim, J. Lee, and J.-H. Oh, "Online free walking trajectory generation for biped humanoid robot KHR-3 (HUBO)," in *Robotics and Automation, 2006. ICRA 2006. Proceedings 2006 IEEE International Conference on*, 2006, p. 1231Ű1236.

[100] M. Vukobratović, B. Borovac, D. Surla, and D. Stokic, *Biped Locomotion*, Berlin, Germany, 1990.

[101] S. H. Collins, A. Ruina, R. Tedrake, and M. Wisse, "Efficient bipedal robots based on passive-dynamic walkers," *Science*, no. 307, pp. 1082–1085, 2005.

[102] M. Raibert, *Legged Robots That Balance*. Cambridge, Mass.: MIT Press, 1986.

[103] M. Ahmadi and M. Buehler, "The {ARL} Monopod {II} Running Robot: Control and Energetics," in *IEEE International Conference on Robotics and Automation*, May 1999, pp. 1689–1694.

[104] G. Zeglin, "The bow leg hopping robot," Ph.D. dissertation, Robotics Institute, Carnegie Mellon University, Pittsburgh, PA, October 1999.

[105] D. Renjewski, "An engineering contribution to human gait biomechanics," Dissertation, TU Ilmenau, Germany, 2012.

[106] J. W. Grizzle, J. Hurst, B. Morris, H. W. Park, and K. Sreenath, "Mabel, a new robotic bipedal walker and runner," in *American Control Conference*, St. Louis, Jun. 2009.

[107] C. T. Farley, J. Glasheen, and T. A. McMahon, "Running springs: Speed and animal size," *Journal of Experimental Biology*, vol. 185, pp. 71–87, 1993.

[108] G. Dalleau, A. Belli, M. Bourdin, and J.-R. Lacour, "The spring-mass model and the energy cost of treadmill running," *European journal of applied physiology and occupational physiology*, vol. 77, no. 3, p. 257Ű263, 1998.

[109] R. Full and D. Koditschek, "Templates and anchors: neuromechanical hypotheses of legged locomotion on land," *J. of Exp. Biol.*, vol. 202, pp. 3325–3332, 1999.

[110] A. Seyfarth and H. Geyer, "Natural control of spring-like running – optimized self-stabilization," in *Proceedings of the 5th international conference on climbing and walking robots*. Professional Engineering Publishing Limited, 2002, pp. 81–85.

[111] R. J. Full, T. Kubow, J. Schmitt, P. Holmes, and D. Koditschek, "Quantifying dynamic stability and maneuverability in legged locomotion," *Integrative and Comparative Biology*, vol. 42, pp. 149–57, 2002.

[112] S. W. Lipfert, M. Günther, D. Renjewski, S. Grimmer, and A. Seyfarth, "A model-experiment comparison of system dynamics for human walking and running," *Journal of Theoretical Biology*, vol. 292, p. 11Ű17, 2012.

[113] H.-M. Maus, S. Lipfert, M. Gross, J. Rummel, and A. Seyfarth, "Upright human gait did not provide a major mechanical challenge for our ancestors," *Nature Communications*, vol. 1, no. 6, pp. 1–6, Sep. 2010.

[114] E. Andrada, J. Nyakatura, R. Müller, C. Rode, and R. Blickhan, "Grounded running: An overlooked strategy for robots," *Autonomous Mobile Systems 2012*, p. 79Ű87, 2012.

[115] R. Blickhan and R. J. Full, "Similarity in multilegged locomotion: bouncing like a monopode," *J. of Comp. Physiol.*, vol. 173, pp. 509–17, 1993.

[116] D. Ferris, M. Louie, and C. Farley, "Running in the real world: adjusting leg stiffness for different surfaces," *Proc. R. Soc. Lond. B Biol. Sci.*, vol. 265, no. 1400, pp. 989–994, 1998.

[117] J. Pratt, J. Carff, S. Drakunov, and A. Goswami, "Capture point: A step toward humanoid push recovery." in *Proceedings of the IEEE-RAS/RSJ International Conference on Humanoid Robots*, 2006.

[118] J. Schmitt and J. Clark, "Modeling posture-dependent leg actuation in sagittal plane locomotion," *Bioinspiration & Biomimetics*, vol. 4, no. 4, p. 46005, 2009. [Online]. Available: http://stacks.iop.org/1748-3190/4/i=4/a=046005

[119] F. Roos, H. Johansson, and J. Wikander, "Optimal selection of motor and gearhead in mechatronic applications," *Mechatronics*, vol. 16, no. 1, pp. 63–72, Feb. 2006.

APPENDICES

Appendix A – ATRIAS–SLIP Model Equivalency

This appendix will analytically prove that the equations of motion of the ATRIAS model generated using the Lagrangian formulation are mathematically equivalent to the spring-mass model equations of motion for vertical hopping.

The spring-mass model we are mapping to the ATRIAS model has the same mass m and leg length l (from the center of mass m to the contact point between the toe and the ground). The independent variables for this equivalent spring-mass model are shown in Figure A.1. These are θ, the angle of the prismatic joint leg to the ground, and l, the leg length. The equations of motion for the SLIP model in polar coordinates are represented as follows [118]:

$$0 = m\ddot{\ell} - m\ell\dot{\theta}^2 + F_{spring} + mg\sin\theta \tag{A.1}$$

$$0 = m\left[\ell^2\ddot{\theta} + 2\ell\dot{\ell}\dot{\theta}\right] + mg\ell\cos\theta \tag{A.2}$$

Where F_{spring} is the spring force which for linear spring is equal to $k_{spring}\Delta\ell$.

The Lagrangian formulation is used for the equations of motion for the ATRIAS model and, for a general dynamical system the Lagrangian equations, are represented as follows:

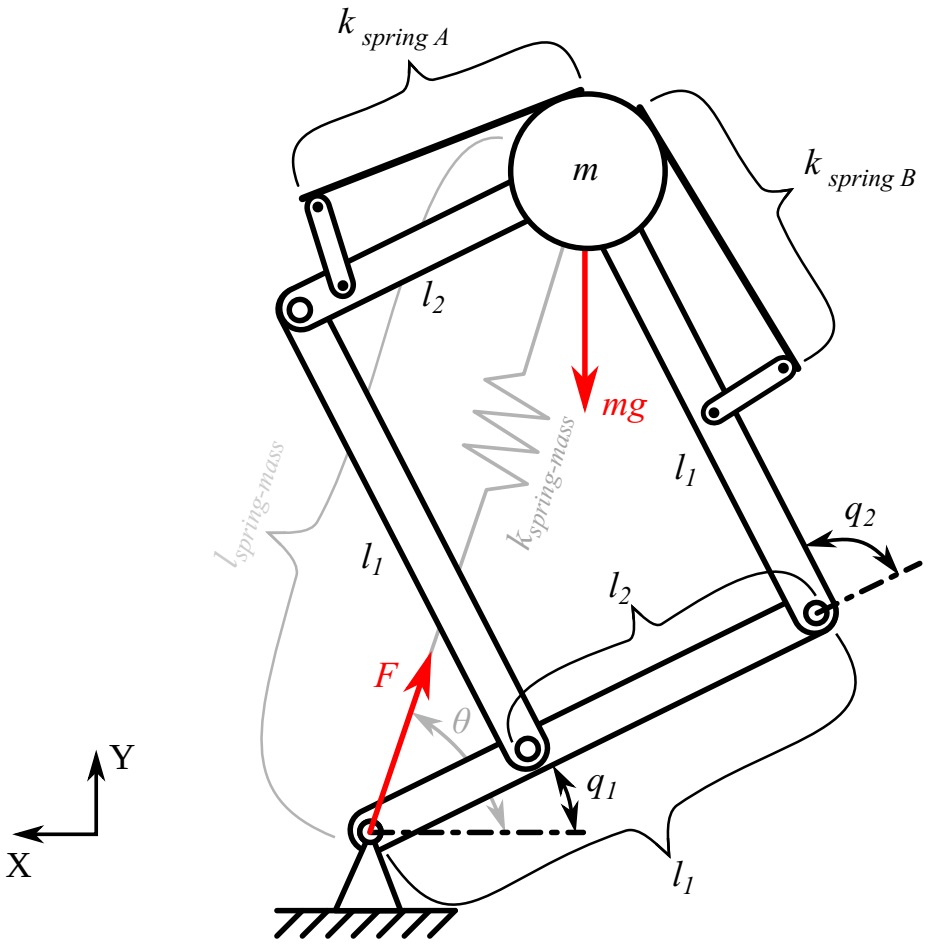

Figure A.1: The ATRIAS model with our chosen variables, q_1 and q_2, for the Lagrangian Formulation in this proof. A geometrically equivalent spring-mass model, and its chosen variables, is overlayed onto the ATRIAS model, shown in gray. The dynamics of these to models are analytically identical for vertical bouncing ($\theta = 0$). Note: the springs are shown as a schematic coil spring, and as such, are not in the appropriate, real world location. See Figure 2.4 for the correct location of the leaf springs.

$$Q_i = \frac{\partial}{\partial t}\left(\frac{\partial \mathcal{L}}{\partial \dot{q}_i}\right) - \left(\frac{\partial \mathcal{L}}{\partial q_i}\right)$$

where $\mathcal{L} = T - V$ with $T = kinetic\ energy$ and $V = potential\ energy$. The generalized coordinates (independent degrees of freedom) are q_i and non-conservative forces along the generalized coordinates are Q_i. For ATRIAS model, the two generalized coordinates are q_1 and q_2 as shown in Figure A.1.

For this evaluation we look at the passive system with no motor input. Realistically this is true when the motors are locked, that is, not contributing any work to the system to keep the system conservative. The base of each spring is clamped to these motor outputs, while the other end is pinned to a linkage that is then pinned to a member of the four-bar linkage giving rotational compliance. In addition, we assume the springs and all mechanical components are ideal and have no frictional or other losses. Therefore the non-conservative forces, Q_i, are zero. Mass of the linkages in the leg are considered negligible compared to the mass located at the hip joint (mass m in Figure A.1).

The point contact of the toe to the ground is assumed to be a pin joint during stance, given a good friction contact. With this we can form the kinetic energy, T and potential energy, V, as follows:

$$T = \frac{1}{2}m\left[(-\ell_1\dot{q}_1\sin q_1 - \ell_1(\dot{q}_1+\dot{q}_2)\cos(q_1+q_2)\right)^2$$

$$
\begin{aligned}
& + (\ell_1 \dot{q}_1 \cos q_1 + \dot{q}_1 + \dot{q}_2 \\
& + \ell_1 (q_1 + q_2) \sin(q_1 + q_2))^2] \qquad \text{(A.3)} \\
V \;=\; & mg \left(\ell_1 \sin q_1 + \ell_1 \sin(q_1 + q_2) \right) \\
& + 0.25k \left(q_2 - q_{20} \right)^2 \qquad \text{(A.4)}
\end{aligned}
$$

Because of the symmetry of the system for vertical bouncing, any deflection in one spring, or change in q_2, will deflect both springs. We represent the neutral position for the springs, or zero deflection, as q_{20}.

Substituting the kinetic energy and the potential energy to Lagrangian equations, we arrive at the two following equations:

$$
\begin{aligned}
0 \;=\; & m \left[\ddot{q}_1 (2\ell_1^2 + 2\ell_1^2 \cos q_2) + \ddot{q}_2 (\ell_1^2 + \ell_1^2 \cos q_2) \right. \\
& \left. - \ell_1^2 \dot{q}_2 (2\dot{q}_1 + \dot{q}_2) \sin q_2 \right] \\
& + mgl_1 \cos q_1 + mgl_1 \cos(q_1 + q_2) \qquad \text{(A.5)} \\
0 \;=\; & m\ell_1^2 \ddot{q}_1 cos q_2 + m\ell_1^2 (\ddot{q}_1 + \ddot{q}_2) \\
& + m\ell_1^2 \dot{q}_1{}^2 \sin q_2 + mg\ell_1 \cos(q_1 + q_2) \\
& + 0.5k(q_2 - q_{20}) \qquad \text{(A.6)}
\end{aligned}
$$

While Equations A.5 and A.6, in this form, do not immediately match the Equations of motion for the SLIP model, Equations A.1 and A.2, we can use the following geometric relations, Equations A.7 and A.8, that relate the general coor-

dinates between the two models and show that they do indeed match analytically. The following are the geometric relations between the generalized coordinates of ATRIAS model and an equivalently sized SLIP model. See Figure A.1 for these two sets of coordinates overlayed onto one another.

$$\theta = q_1 + \frac{q_2}{2} \tag{A.7}$$

$$\ell = 2\ell_1 \cos\left\{\frac{q_2}{2}\right\} \tag{A.8}$$

Combining the ATRIAS Equations by the formula $(equation\ A.6) - \frac{1}{2}(equation\ A.5)$ and commonly known trigonometric identities and the substitutions of Equations A.7 and A.8 we arrive at Equation A.2. However, this equation can be ignored for the case of vertical bouncing considered in this analysis, as Equation A.2 is zero when the leg is vertical; when $\theta = 90°$ and $\ddot{\theta} = \dot{\theta} = 0$.

With substitution of Equations A.7 and A.8 and derivatives thereof into Equation A.5, we arrive at Equation A.1, with one difference: the behavior of the spring. For the conventional SLIP model the spring is a simple, linear spring with spring constant k and the force from this spring is can be assumed as $F_{spring} = k\Delta\ell$. If the springs in the ATRIAS model are linear, the effective leg spring function due to the 4-bar leg linkage is:

$$F_{spring} = \frac{k}{2\ell_1 \sin(\frac{q_2}{2})}(q_2 - q_{20}). \tag{A.9}$$

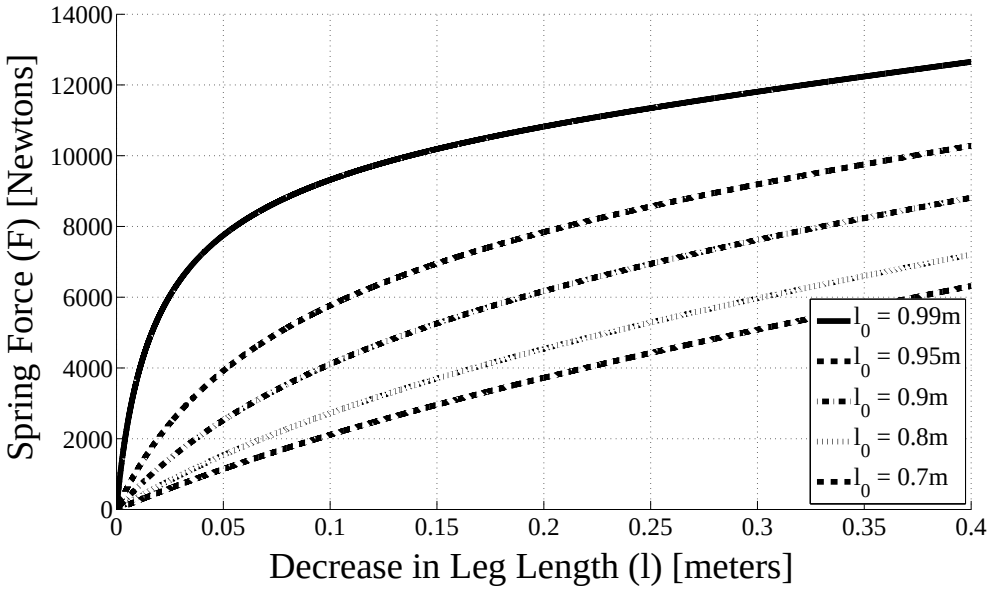

Figure A.2: Net force response at toe, or hip joint (they are equivalent), due to increasing spring deflection on ATRIAS model. When $L_0 = 0.99$m it is clearly visible that the system exhibits the behavior of a softening spring. This trend is consistent for all curves shown on this plot. The ATRIAS model with linear springs is analytically equivalent to a SLIP model with softening springs. Note: we do *not* use $L_0 = 1.0$m because this initial condition is a singularity of the system.

With linear leaf springs with stiffness k on the ATRIAS model we plot the force at the toe due to increasing spring deflections for a selection of leg lengths, Figure A.2. When the leg is straighter $L_0 = 1.0$m or 0.9m we clearly see that the curve indicates a softening spring, a trend that is consistent among all curves in Figure A.2, when in fact the leaf physical springs in use are linear. Therefore, the ATRIAS model can be mapped to a spring-mass model with a softening spring of Equation A.9.

This proves that the planar ATRIAS model is not an approximation of the SLIP model for vertical bouncing but is in fact analytically identical given our reasonable, simple case assumptions.

Appendix B – ATRIAS 2.1 Actuator Power Profile

In this section a representative example gait is used to identify ATRIAS' typical, main *actuator power profile*. ATRIAS' load scenario is given through its four main actuator velocities, their in-series spring/actuator torques, and the measured power. The gait is a walking gait with a speed of 0.85 m/s, the mean data of 12 consequtive recorded steps was applied here. A motor model similar to [119] was implemented to fill gaps from non-measurable, otherwise missing dynamical motor characteristics. Power "components", such as ratio of regeneration, electrical power losses, and individual motor powers were non-measurable, mostly because they were not accessible in the ATRIAS setup. Only the instantaneous summed power of all four actuators could be measured by a power clamp. Consequently, the here presented ATRIAS motor model provides otherwise unaccessible system parameters such as *a*) instantaneous power applied to accelerate actuators, *b*) electrical power losses, *c*) actuator efficiencies, *d*) and the instantaneous regeneration of actuators and amplifiers. The model further allows to precisely look at swing and stance phase power characteristics of the ATRIAS system.

B.1 Experimental Setup

Full dynamics in a legged robotic system can be derived if both kinematic and dynamic data is available. ATRIAS allows to calculate its actuator's instantaneous load continuously during swing and stance phase. Axial leg forces, and tangential leg torques were measured indirectly through the robot's deflecting leg springs, one for each of ATRIASâĂŹ leg motors (Section **??**). Leg forces and torques are derived through the robots kinematics and the measured actuator forces and torques (Equation. In a system without internal actuator torque estimation, swing phase dynamics cannot be estimated. Few robots are equipped with a full set of joint torque sensors, and only sparse data of robot swing phase dynamics is available from literature. ATRIAS's internal leg dynamic measurements directly enable us to measure those values, and apply them in the motor model to gain insights into details of the system's motor power. All sensor data was recorded at a sampling frequency of 1000 Hz. The data of the walking ATRIAS robot was recorded over 12 full locomotion cycles. A full cycle was arbitrarily defined between the beginning of the left leg swing phase, and the end of the left leg stance phase. The average gait cycle time was 1.1sec, at a gait cycle duty factor of 0.6 (Figure B.1, stance duration per gait cycle). The motor-torque crossing from loaded to unloaded, of the left leg motor-B, was used to define the onset of swing phase, and the end of stance phase again. All cycles were cut manually, and trajectories were interpolated with 1000 samples.

B.2 Motor model

We implemented a variant of the motor model by [119], for each of ATRIAS' four main actuators. We extended Roos' motor model with the capability of identifying actuators in generator mode; in phases of negative power, those actuators would push electrical power back into the robot's electrical grid. We found that this regenerated power was almost always instantly re-used, by one of the other motors.

Motor power P_m is described as sum of electrical losses P_elec and mechanical losses P_mech [119, equation 10-13]. Mechanical losses depend on the instantaneous power applied through the load (T_l, $\dot{\theta}_\mathrm{l}$) and through accelerating the motor and gear components (J_m motor inertia, J_g gearbox inertia).

$$P_\mathrm{m} = P_\mathrm{elec} + P_\mathrm{mech} \tag{B.1}$$

$$P_\mathrm{mech} = (J_\mathrm{m} + J_\mathrm{g})\ddot{\theta}_\mathrm{l}\dot{\theta}_\mathrm{l}n^2 + \frac{T_\mathrm{l}}{\mu_\mathrm{g}}\dot{\theta}_\mathrm{l} \tag{B.2}$$

$$P_\mathrm{elec} = R_\mathrm{m}I^2 = R_\mathrm{m}\frac{T_\mathrm{m}^2}{k_\mathrm{T}^2} \tag{B.3}$$

θ_l indicates the position of the load, here the actuator position in [rad], $\dot{\theta}_\mathrm{l}$ its velocity and $\ddot{\theta}_\mathrm{l}$ its acceleration. T_l in [Nm] is the load torque measured through spring deflection, μ_g is the approximation of the harmonic drive gearbox efficiency. Electrical losses are calculated through the motor winding resistance (R_m in [Ω]), and the motor coefficient k_T. n is the gear ratio of the harmonic drive. We externally measured ATRIAS' electrical power P_clamp and compared it to the model-predicted motor power $P_\mathrm{m,robot}$, as sum of its four main leg actuators [motor ID's: (L) left

and (R) right side, A and B motor]:

$$P_{\mathrm{m,robot}} = P_{\mathrm{m,LA}} + P_{\mathrm{m,LB}} + P_{\mathrm{m,RA}} + P_{\mathrm{m,RB}} \tag{B.4}$$

Other than in Roos' model the ATRIAS actuator and amplifiers apply an imperfect generator mode, in case of negatively applied power. Only externally applied loads, or load through acceleration can produce negative power (equation B.2):

$$P_{\mathrm{mech,regen,motorID}} = -\mu_{\mathrm{regen}} P_{\mathrm{mech,motorID}} \tag{B.5}$$

We identified the efficiency of regeneration between $\mu_{\mathrm{regen}} = 30\,\%$ and $40\,\%$.

B.3 Results

The average, minimal and maximal leg forces and leg torques per full gait cycle of this example gait are given in Figure B.1 (top and bottom, respectively). The leg force profile shows the walk-gait specific double hump profile, with a maximum leg force of 650 N. Leg torques reached from $-130\,\mathrm{Nm}$ up to $100\,\mathrm{Nm}$, and showed much higher variations, compared to the robot's leg forces (Figure B.1).

Quantitative results from the ATRIAS motor model are presented in Table B.1, separated by stance phase values ($40\,\%$ of cycle time), swing phase values, and full cycle values (1.1 sec in average). The motor model is based on individual sensor data of the left and right ATRIAS leg, and indicates that both legs are not working completely symmetrical. Because the robot is walking in a circle, forces and

torques applied are different between its inner (left) and outer (right) leg. Here shown are only motor model power values for the leg robot leg. Power values are provided, hence the mean of stance and swing, weighted by the duty factor, gives the full cycle power values. The externally applied load ($P_{\mathrm{l,A}}$ and $P_{\mathrm{l,B}}$) during stance phase is caused by impact and weight of the robot, and during swing phase by the mass and inertia of the legs ($P_{\mathrm{l,AB,swing}} \approx 15\,\mathrm{W}$). Swing power values are very low, because the low-weight leg design of ATRIAS. During stance phase motor-A shows a large positive power consumption $P_{\mathrm{l,A,stance}} = 273\,\mathrm{W}$, as it is carrying the robot. Motor-B is showing an almost equally large, but negative power, because the direction of torque is opposite to that of motor A (four-bar construction), while the direction of movement is identical (backwards). Parts of this negative power are being pushed back through the amplifiers, into other, power-draining motors ($P_{\mathrm{regen,B,stance}} = -57\,\mathrm{W}$). As a consequence of a large stance phase torque at lower motor speed, the electrical power losses of motor-A are significant: $P_{\mathrm{elec,A,stance}} = 99\,\mathrm{W}$, or almost 1/3 of the load power. Mechanical swing phase power (instantaneous sum of load and acceleration) is roughly equal between motor-A and motor-B actuators. Though leg masses are low, both actuators require larger accelerations during swing phase, which is 20 % shorter than the robot's stance phase. Further, leg length is altered in addition to the swing-forward movement, what adds an additional acceleration component to the actuators. For the full cycle and both legs, the motor model predicts an electrical power consumption of $P_{\mathrm{m}} = 546\,\mathrm{W}$, versus a measured power consumption of $P_{\mathrm{clamp}} = 567\,\mathrm{W}$. For the 60 kg ATRIAS system, this corresponds to an electrical (metabolic) cost of

transport of 1.13, for this gait.

Table B.1: P_{m} indicates the cummulative, modeled motor power (Equation B.1), P_{mech} the modeled, instantaneous sum of the external load power P_{l} and the internal load power P_{acc} (both with positive and negative values). Latter is caused by the acceleration of motor and gearbox components. Swing time of this gait covers approximatively 40 %. The externally measured power, over all four motors, is shown as P_{clamp}.

Power Type	Motor	Side	Swing	Stance	Full
P_{m}	A	L	135	363	265
P_{m}	B	L	119	-57	19
P_{m}	ABAB	LR	584	517	546
P_{mech}	A	L	151	265	216
P_{mech}	B	L	157	0	67
P_{mech}	ABAB	L	606	510	551
P_{l}	A	L	14	273	162
P_{l}	B	L	16	-268	-146
P_{l}	ABAB	LR	19	22	21
P_{acc}	A	L	12	-9	0
P_{acc}	B	L	-31	25	1
P_{acc}	ABAB	LR	-24	20	1
P_{elec}	A	L	20	99	65
P_{elec}	B	L	13	0	6
P_{elec}	ABAB	LR	137	128	132
P_{regen}	A	L	-36	0	-15
P_{regen}	B	L	-51	-57	-55
P_{regen}	ABAB	LR	-159	-121	-137
P_{clamp}	ABAB	LR	559	573	567

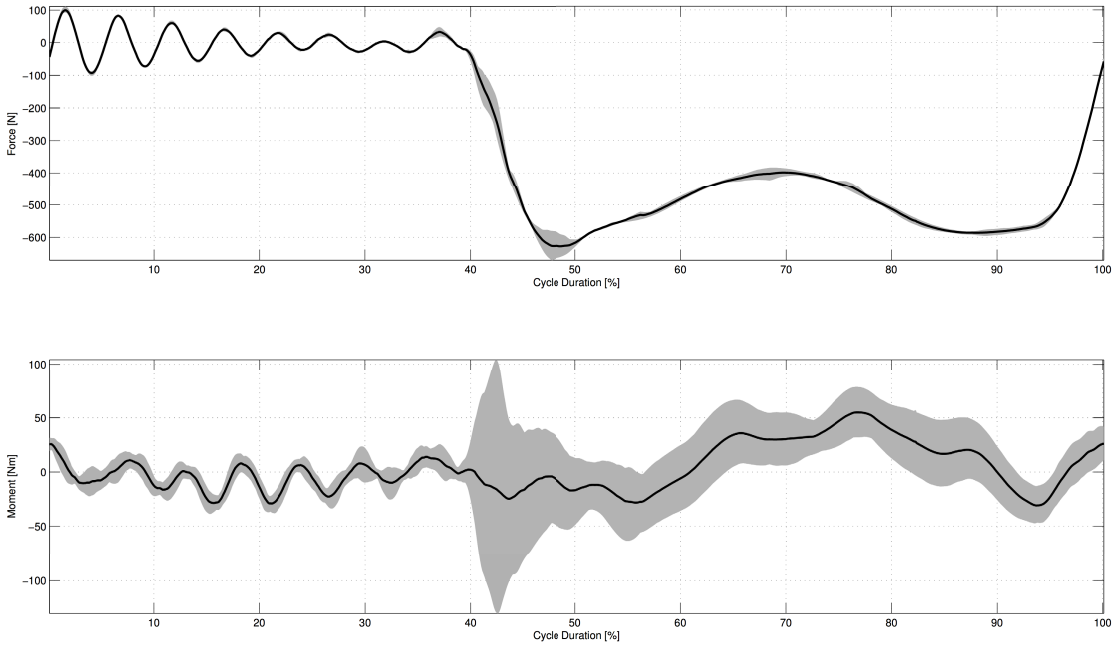

Figure B.1: ATRIAS' leg forces (top) and leg torques (bottom), x-values are normalized by a full gait cycle of a walking gait with an average forward speed of 0.85 m/s. Values of the left leg only are shown. The plot starts with the swing phase, stance phase begins at 40 % of the gait cycle. Continues, bold lines show average force and torque values over 12 strides, grey shaded areas indicate the maximum and minimum band. Maximum leg forces during the walking experiment were around 650 N. Stance phase of the leg torques indicates an initial breaking phase (average −25 Nm), followed by a longer pushing phase (average 55 Nm), and a final, short breaking torque burst (−30 Nm). Strong oscillations of the leg in swing phase are visible both as leg forces, and as leg torque during the first 40 % of the gait cycle.